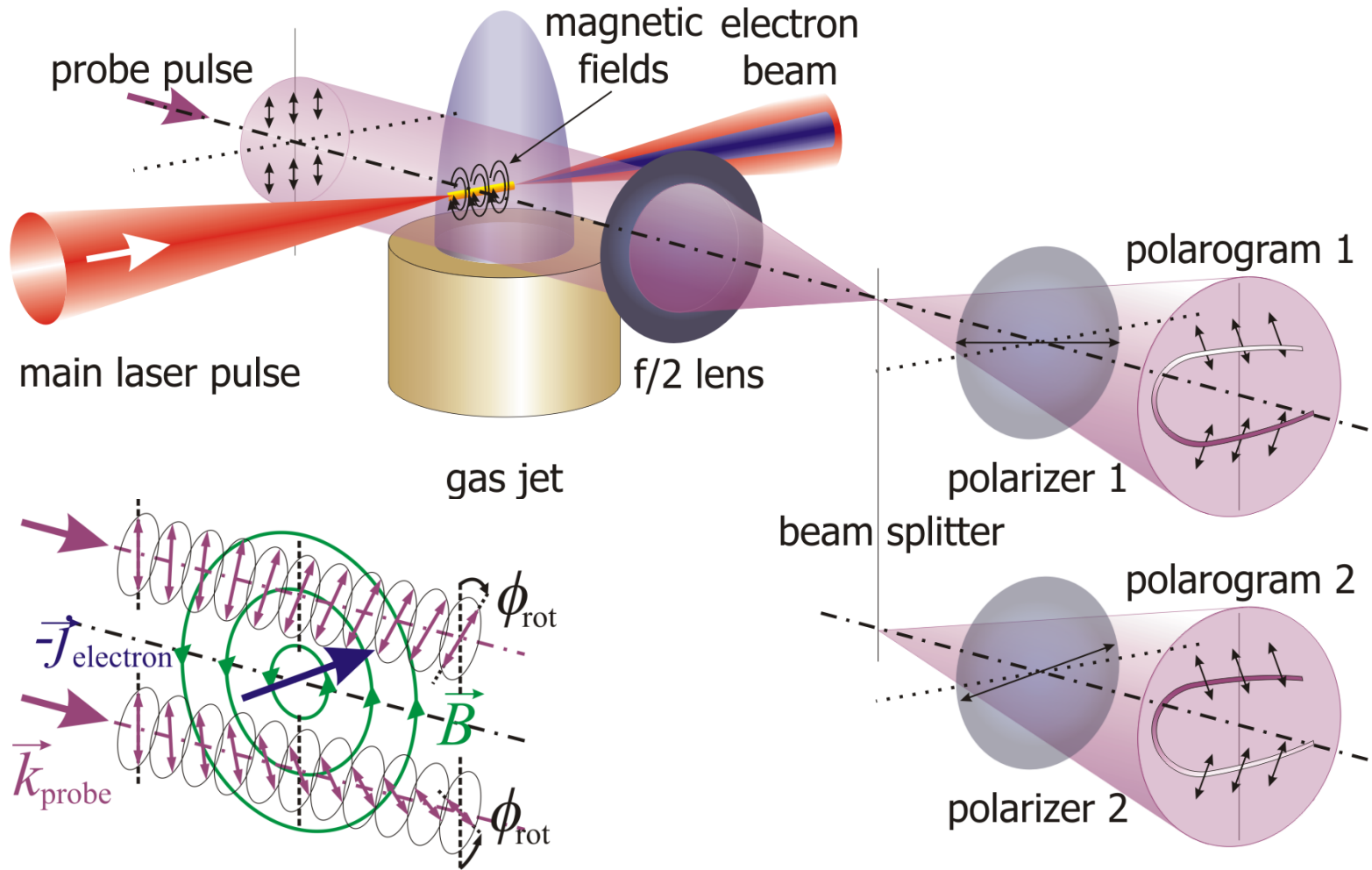




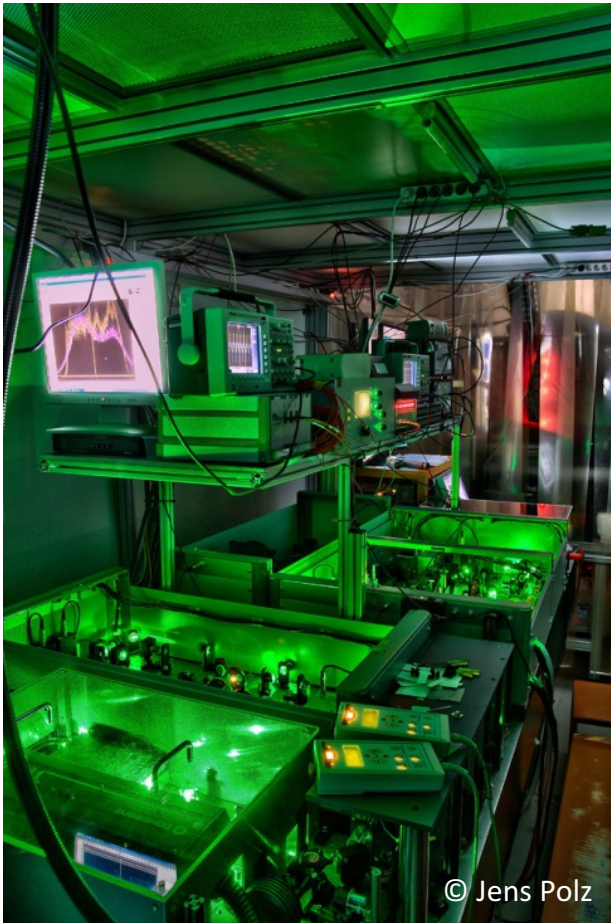
# Electromagnetic Probe Pulses

## Probing of plasma wakefield acceleration process



# Electromagnetic Probe Pulses

## Probing of plasma wakefield acceleration process



Frontend of the JETi laser



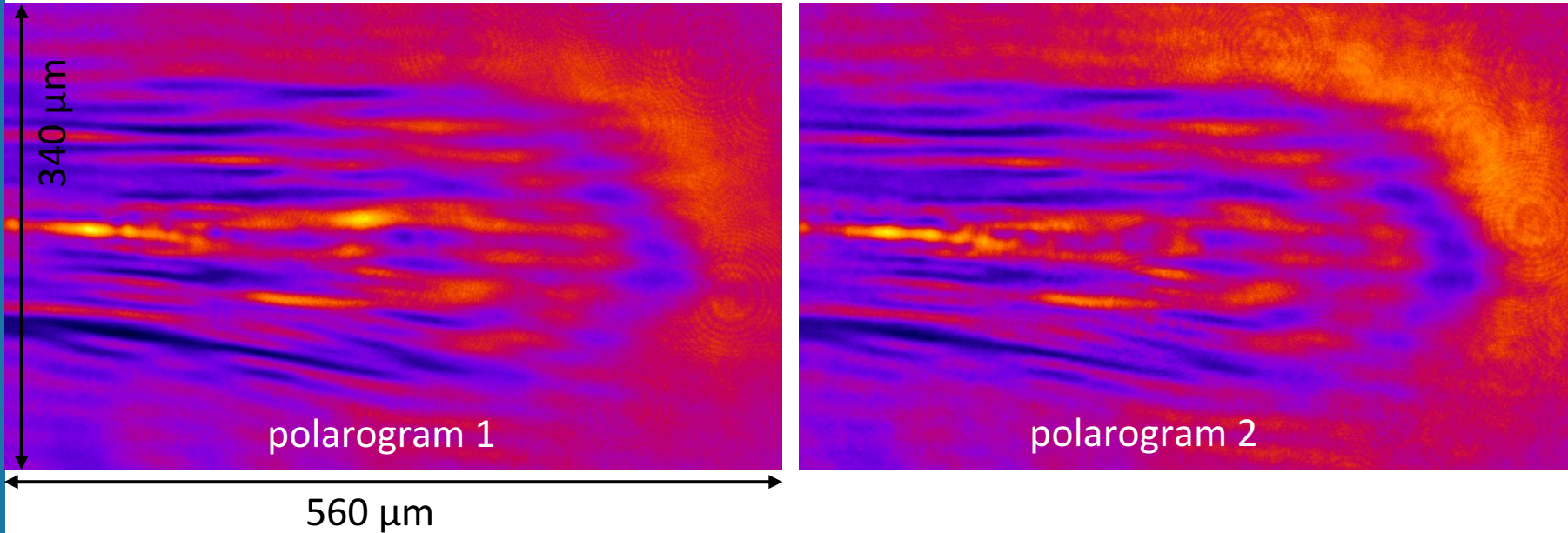
Power amplifier of the JETi laser

85 fs, 850 mJ, (10 TW peak power),  $1 \times 10^{20}$  W/cm<sup>2</sup> peak intensity, 10 Hz

# Electromagnetic Probe Pulses

## Probing of plasma wakefield acceleration process

Two polarograms from two (almost) crossed polarizers:



$$I_{\text{pol1}} = I_0 [1 - \beta_1 \sin^2(90^\circ - \theta_{\text{pol1}} - \phi_{\text{rot}})] \quad I_{\text{pol2}} = I_0 [1 - \beta_2 \sin^2(90^\circ + \theta_{\text{pol2}} - \phi_{\text{rot}})]$$

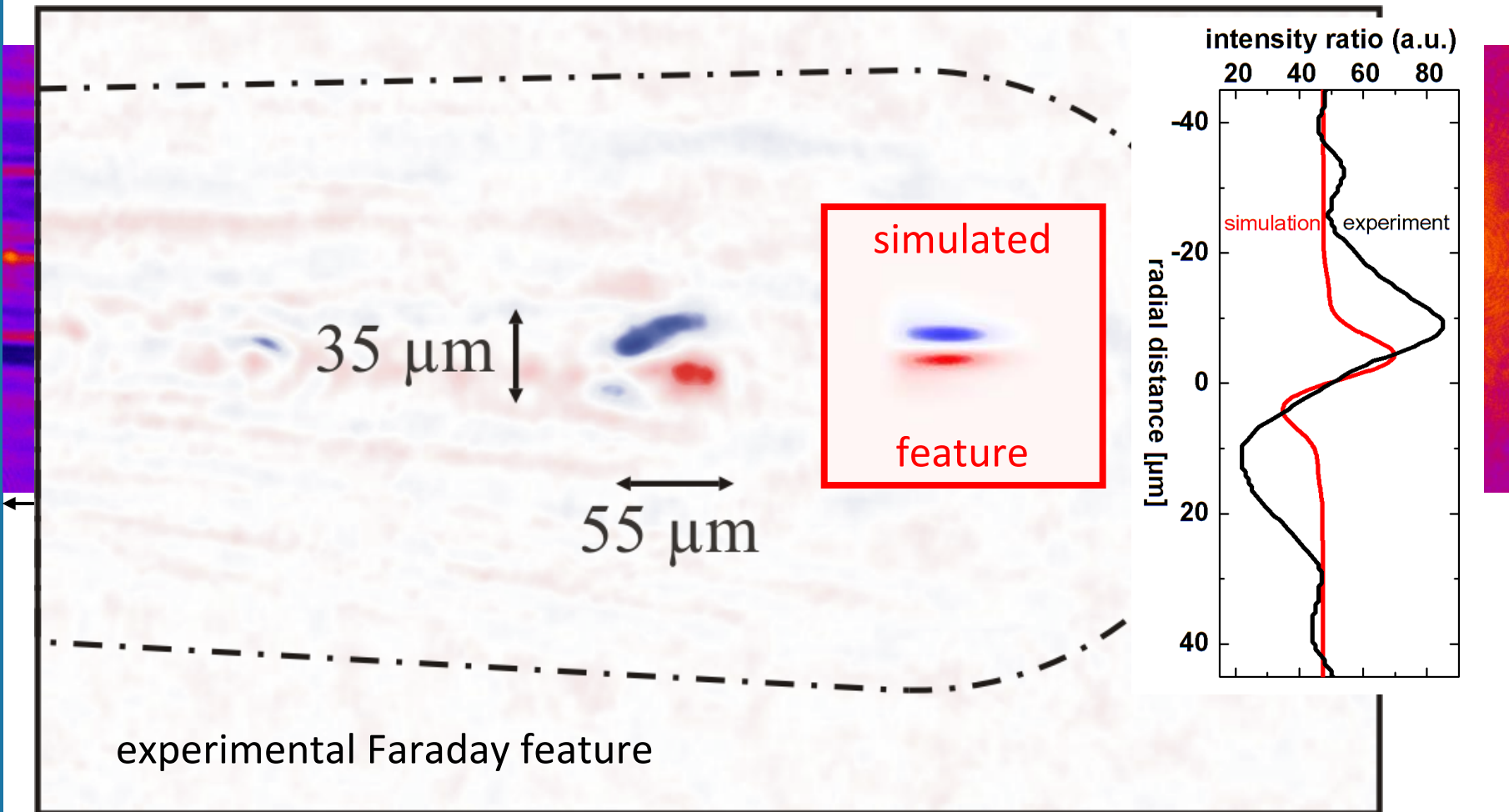
Deduce rotation angle  $\phi_{\text{rot}}$  from pixel-by-pixel division of polarogram intensities:

$$I_{\text{pol1}}(x, y) / I_{\text{pol2}}(x, y)$$



# Electromagnetic Probe Pulses

## Probing of plasma wakefield acceleration process



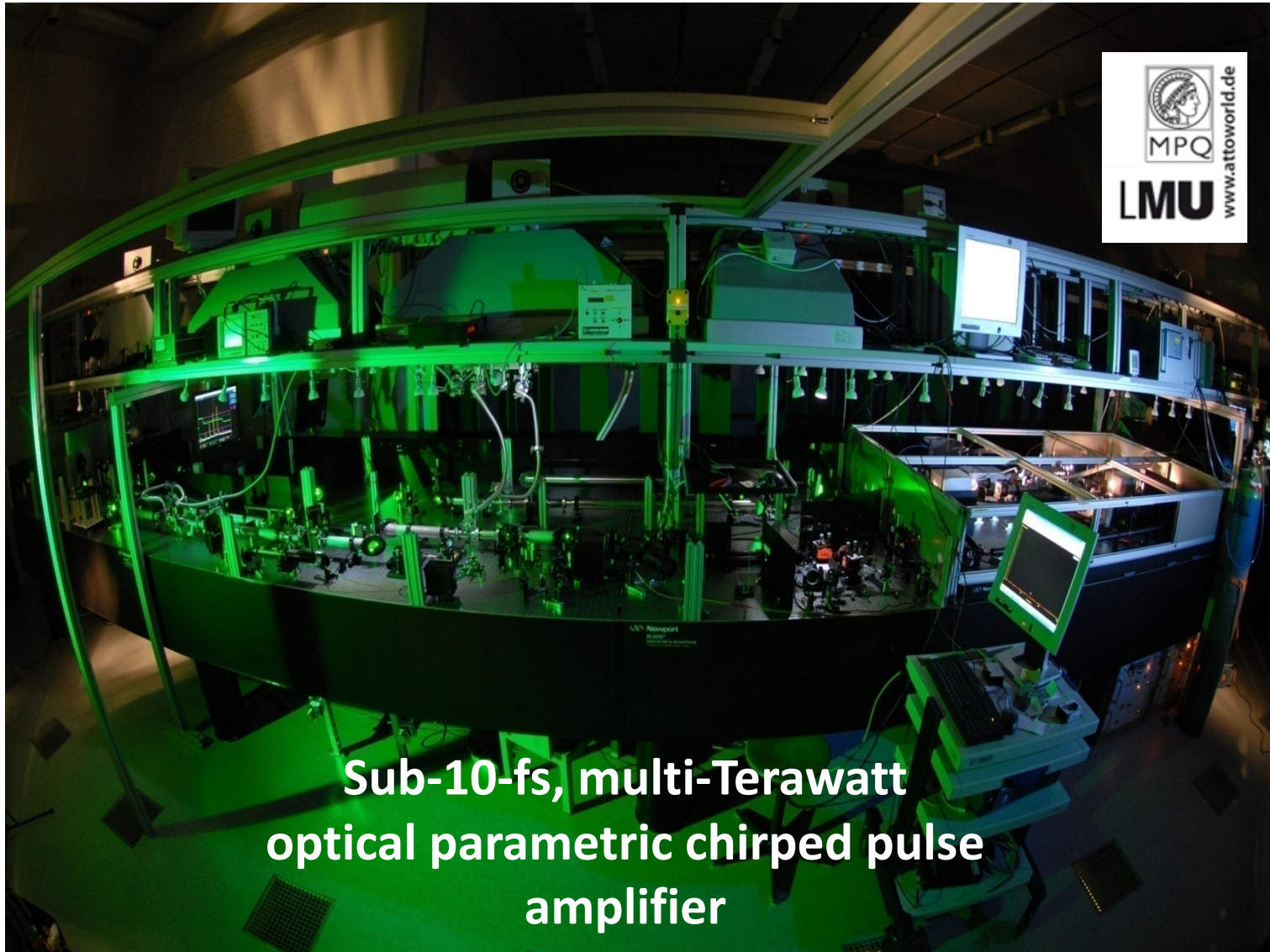
**Experimental evidence for B-fields from MeV electrons and bubble!**

MCK *et al.*, Physical Review Letters **105**, 115002 (2010)



# Electromagnetic Probe Pulses

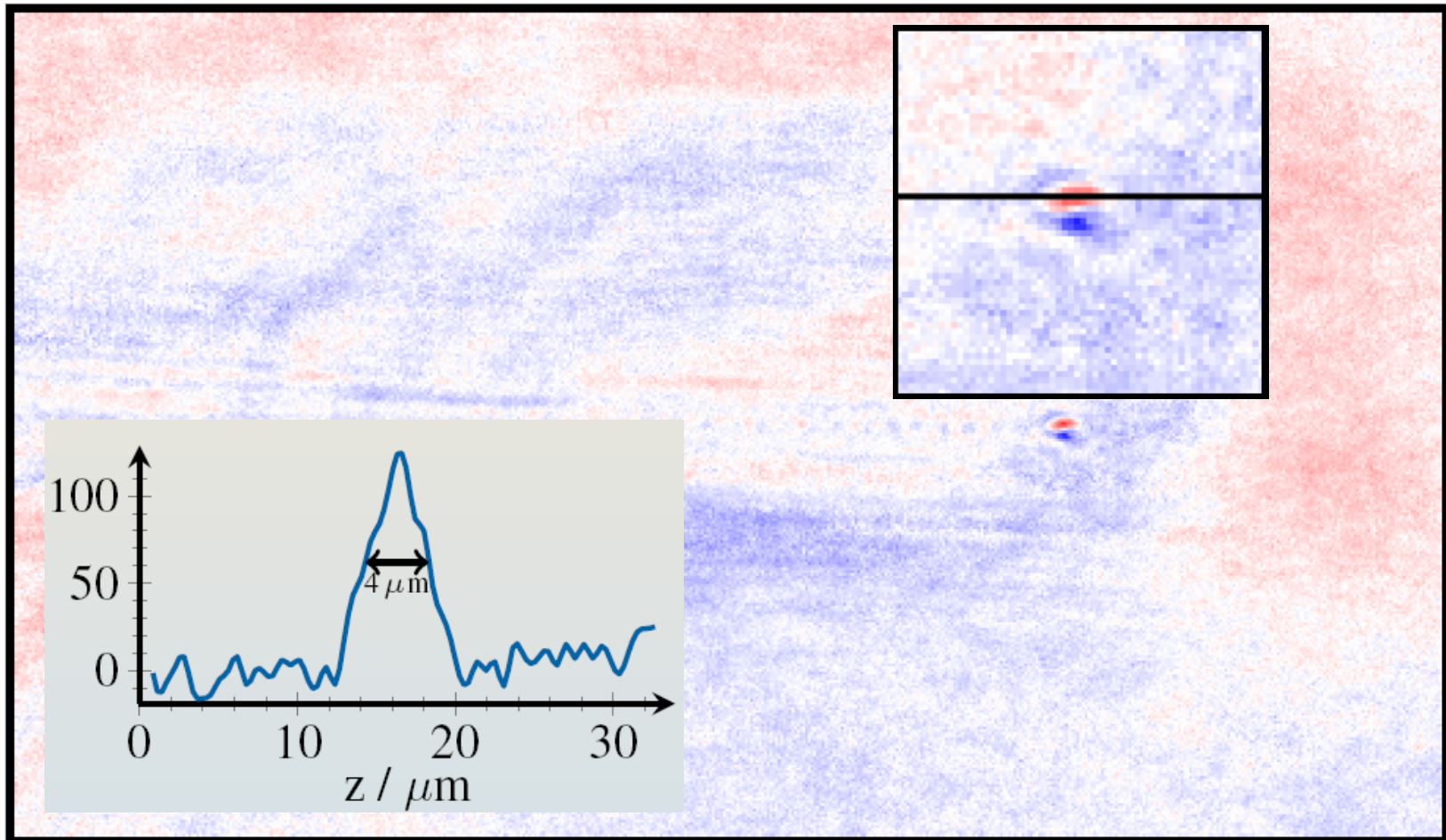
## Probing of plasma wakefield acceleration process



**Sub-10-fs, multi-Terawatt  
optical parametric chirped pulse  
amplifier**

# Electromagnetic Probe Pulses

## Probing of plasma wakefield acceleration process



Electron bunch length:  $\Delta z = 4 \mu\text{m}$

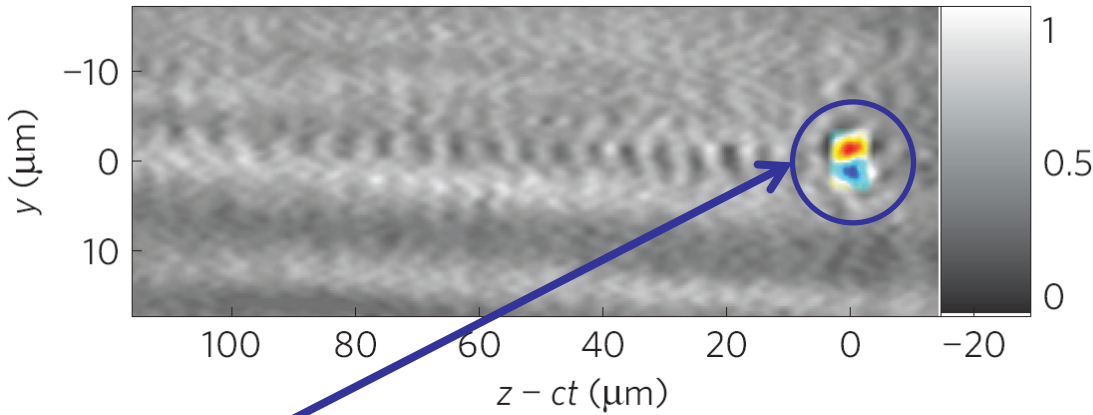
$\tau_{\text{FWHM}} = (6 \pm 2) \text{ fs}$ ,  $\tau_{\text{RMS}} = (2.5 \pm 0.9) \text{ fs}$

A. Buck *et al.*, Nature Physics **7**, 543 (2011)

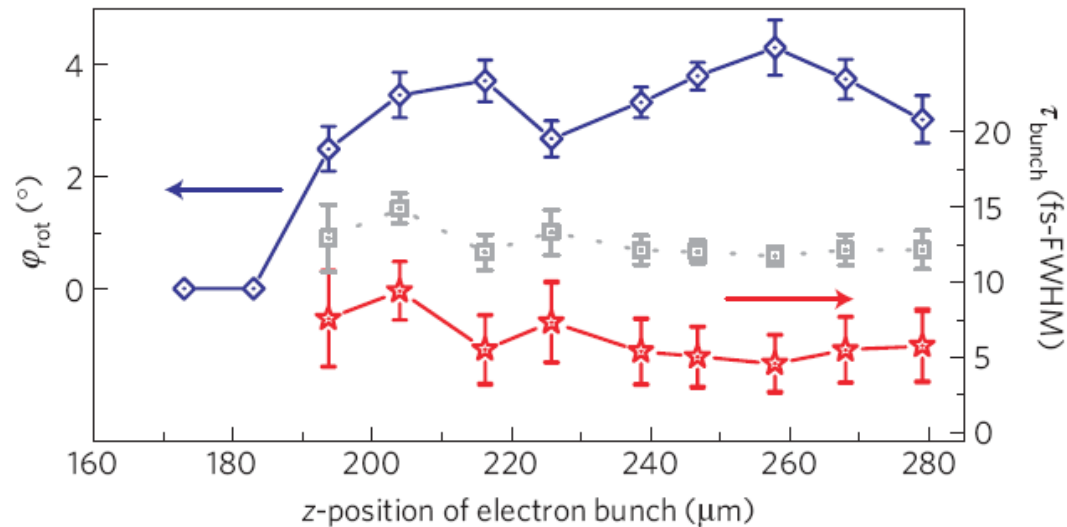


# Electromagnetic Probe Pulses

## Probing of plasma wakefield acceleration process



- **Polarimetry:**  
visualize e-bunch via associated B-fields
- change delay between pump and probe  
⇒ movie of e-bunch formation



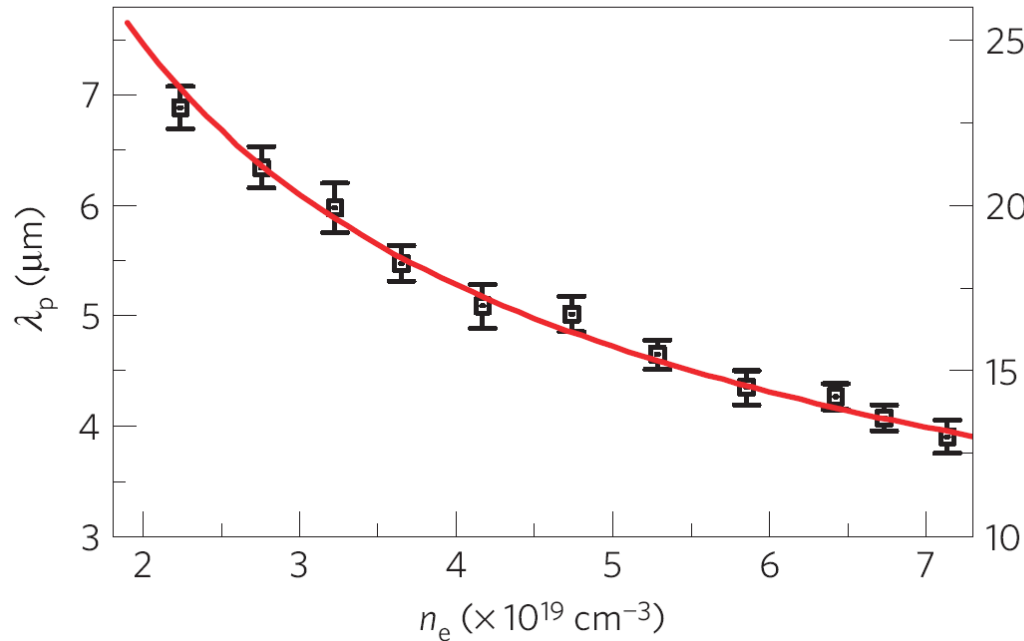
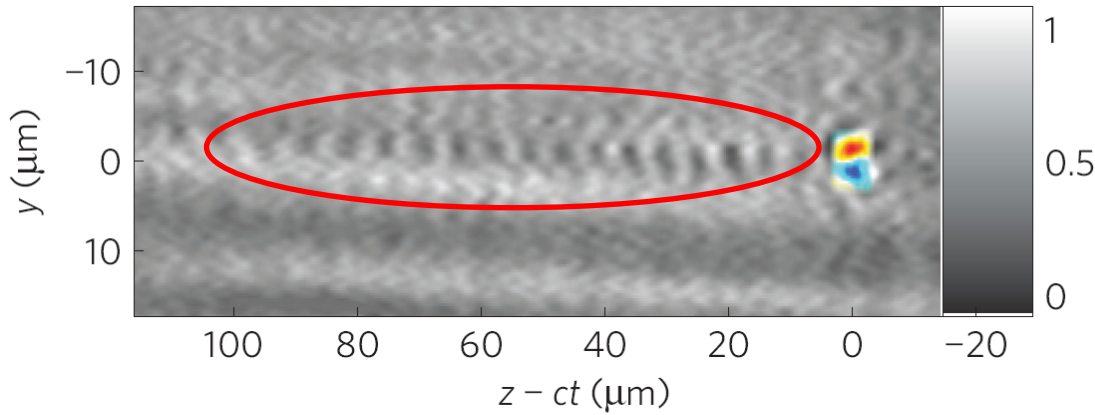
- observe e-bunch formation on-line!

A. Buck *et al.*, Nature Physics **7**, 543 (2011)



# Electromagnetic Probe Pulses

## Probing of plasma wakefield acceleration process



- **Shadowgraphy:**  
visualize plasma wave
- change electron density  $\Rightarrow$   
change plasma wavelength

$$\lambda_p = v_{\text{ph}} T_p \approx \frac{2\pi c}{\omega_p} = 2\pi c \sqrt{\frac{\epsilon_0 m_e}{n_e e^2}}$$

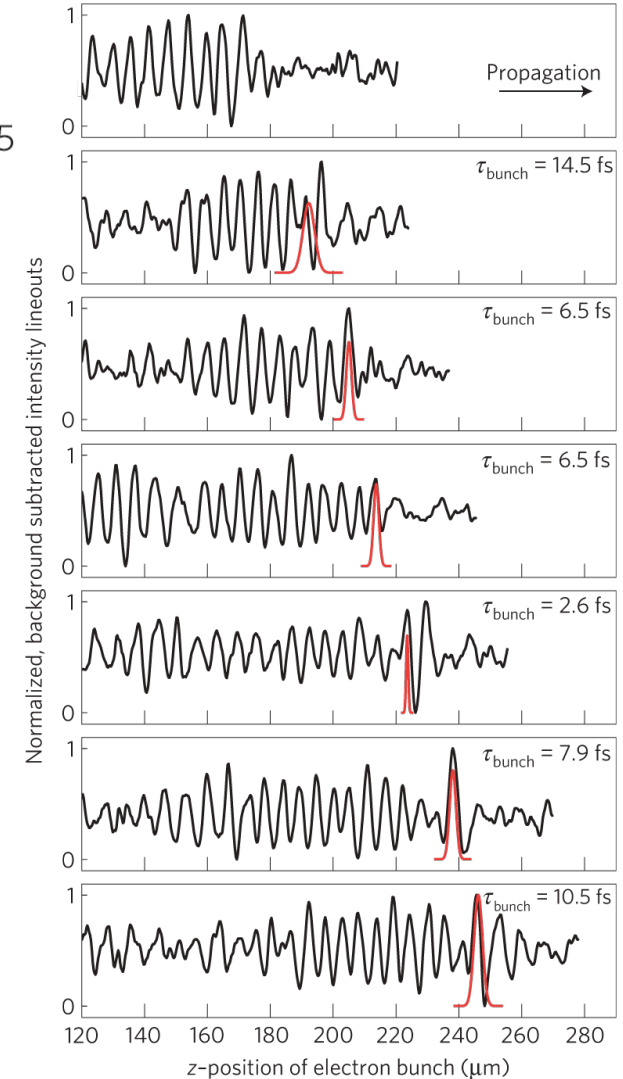
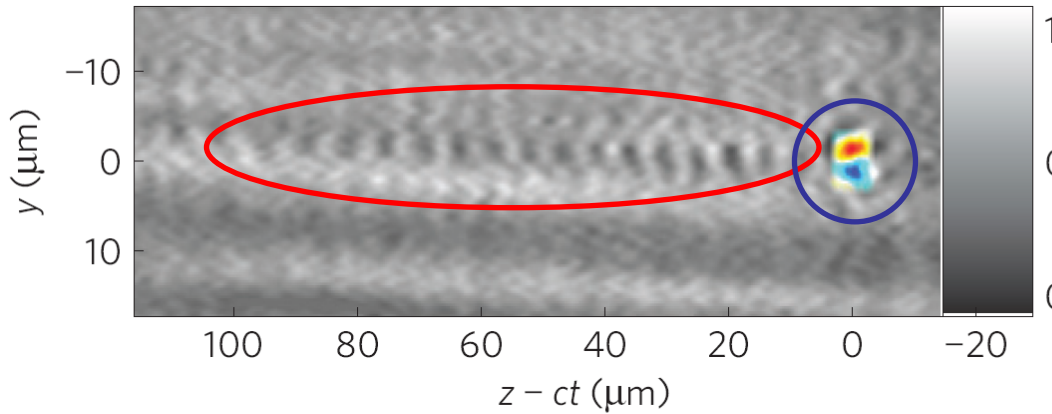
A. Buck *et al.*, Nature Physics **7**, 543 (2011)





# Electromagnetic Probe Pulses

## Probing of plasma wakefield acceleration process



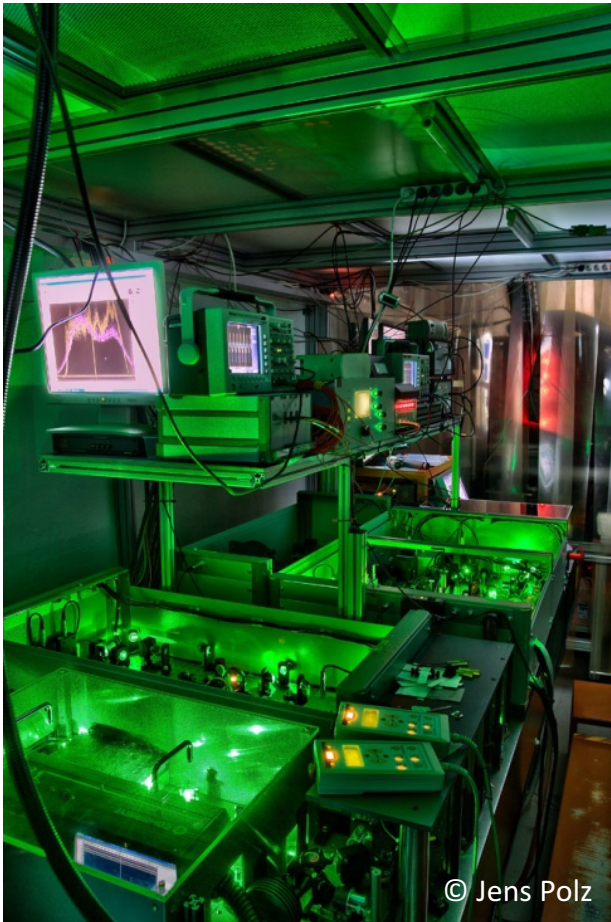
- **Polarimetry + Shadowgraphy:**

Locate position of accelerated electron bunch in the plasma wave

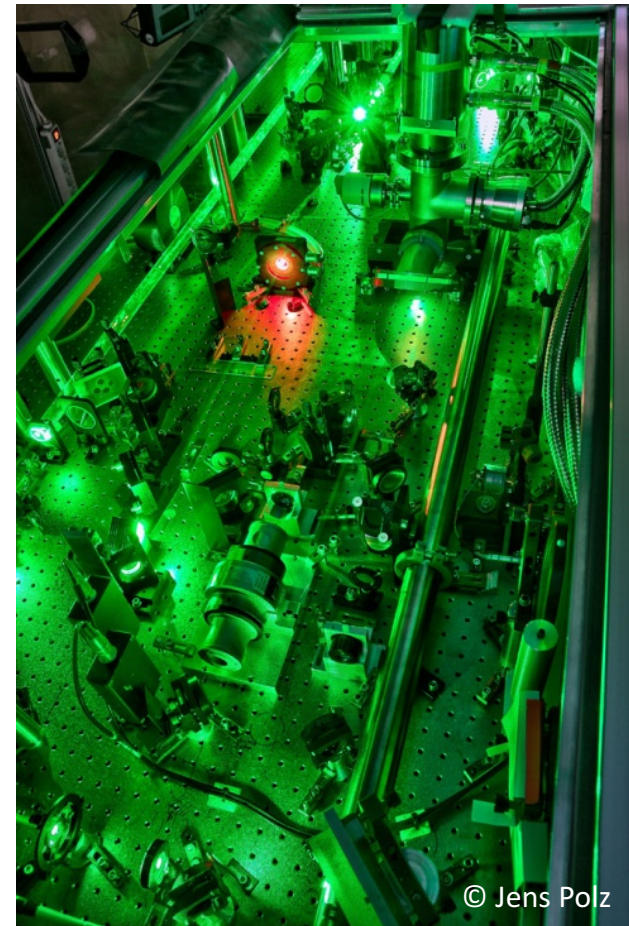
Accelerated electron bunch is situated within the first plasma-wave oscillation

# Electromagnetic Probe Pulses

## Probing of plasma wakefield acceleration process



Frontend of the JETi laser



Power amplifier of the JETi laser

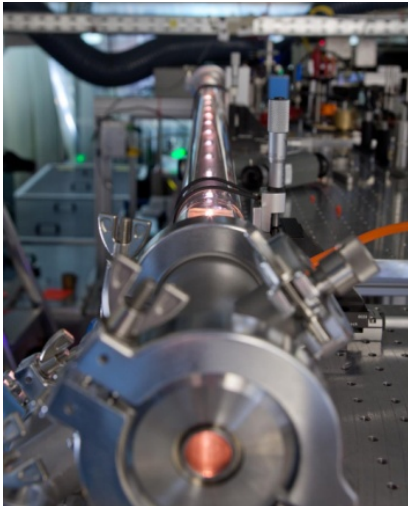
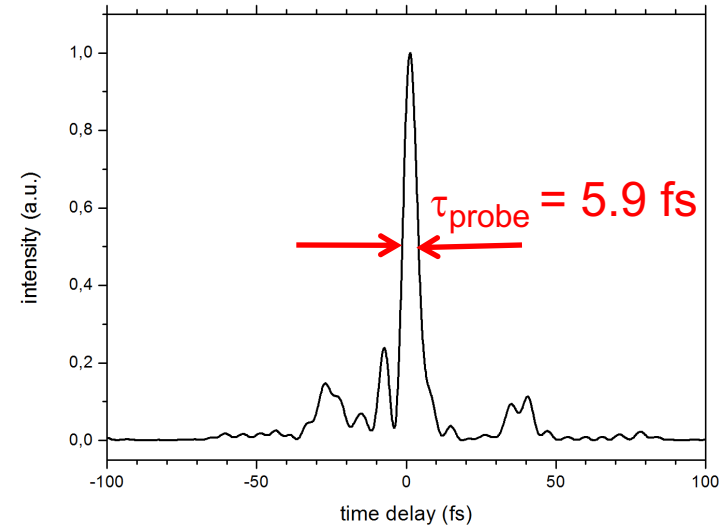
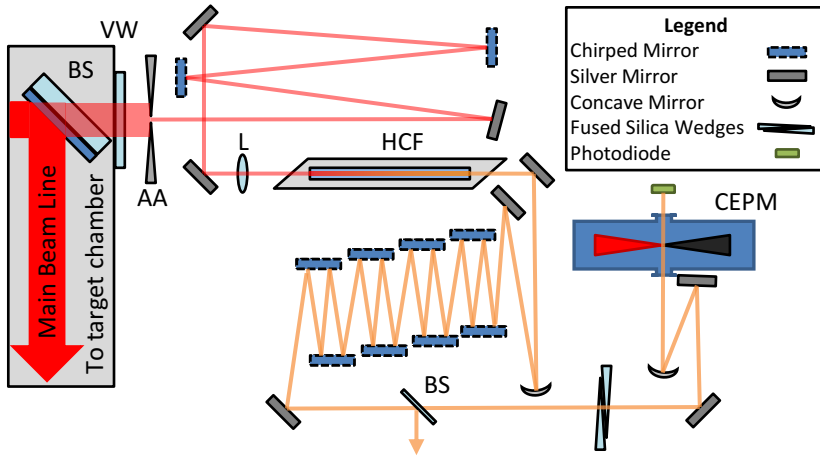
30 fs, 850 mJ, (30 TW peak power),  $3 \times 10^{20}$  W/cm<sup>2</sup> peak intensity, 10 Hz



# Electromagnetic Probe Pulses

## Probing of plasma wakefield acceleration process

- Few-cycle probe pulse generation at JETI via **frequency-broadening**



input pulses from JETI: 32 fs, ~1 mJ

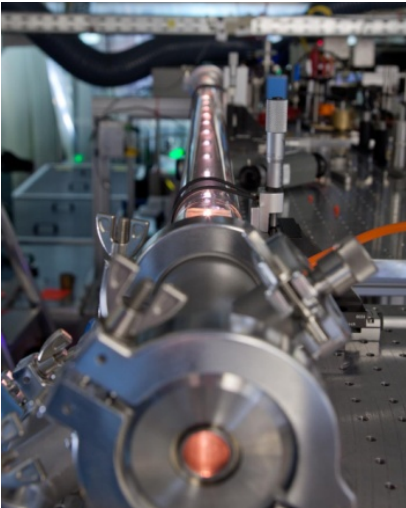
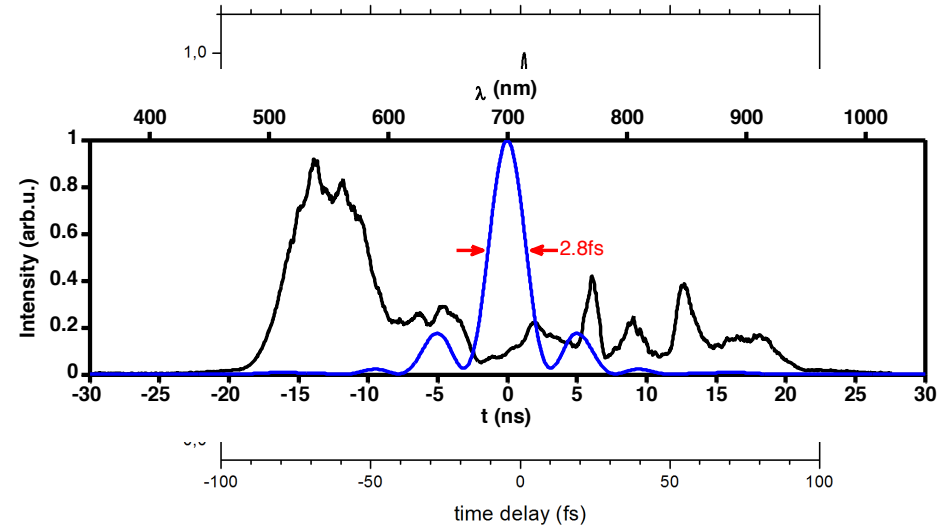
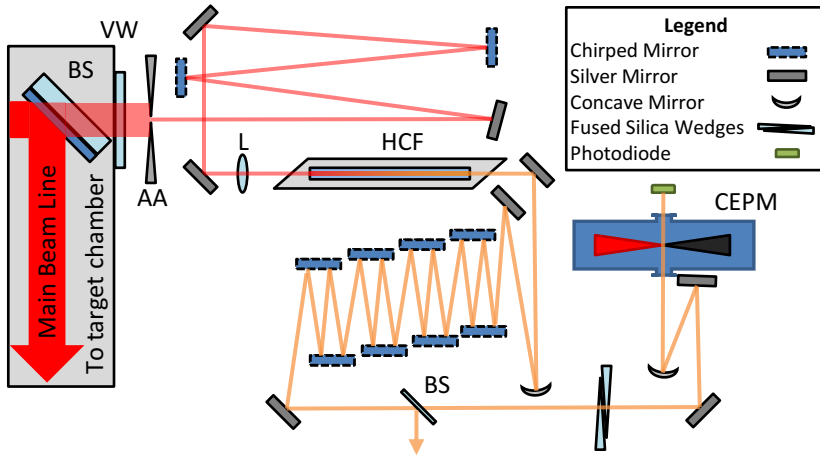
⇒  $(5.9 \pm 0.4)$  fs @ 300  $\mu$ J,

⇒ sufficient for shadowgraphy, Faraday-rotation, interferometry, ...

# Electromagnetic Probe Pulses

## Probing of plasma wakefield acceleration process

- Few-cycle probe pulse generation at JETI via **frequency-broadening**



input pulses from JETI: 32 fs, ~1 mJ

⇒  $(5.9 \pm 0.4)$  fs @ 300  $\mu$ J,  $(2.8 \pm 0.4)$  fs @ 200  $\mu$ J

⇒ sufficient for shadowgraphy, Faraday-rotation, interferometry, ...

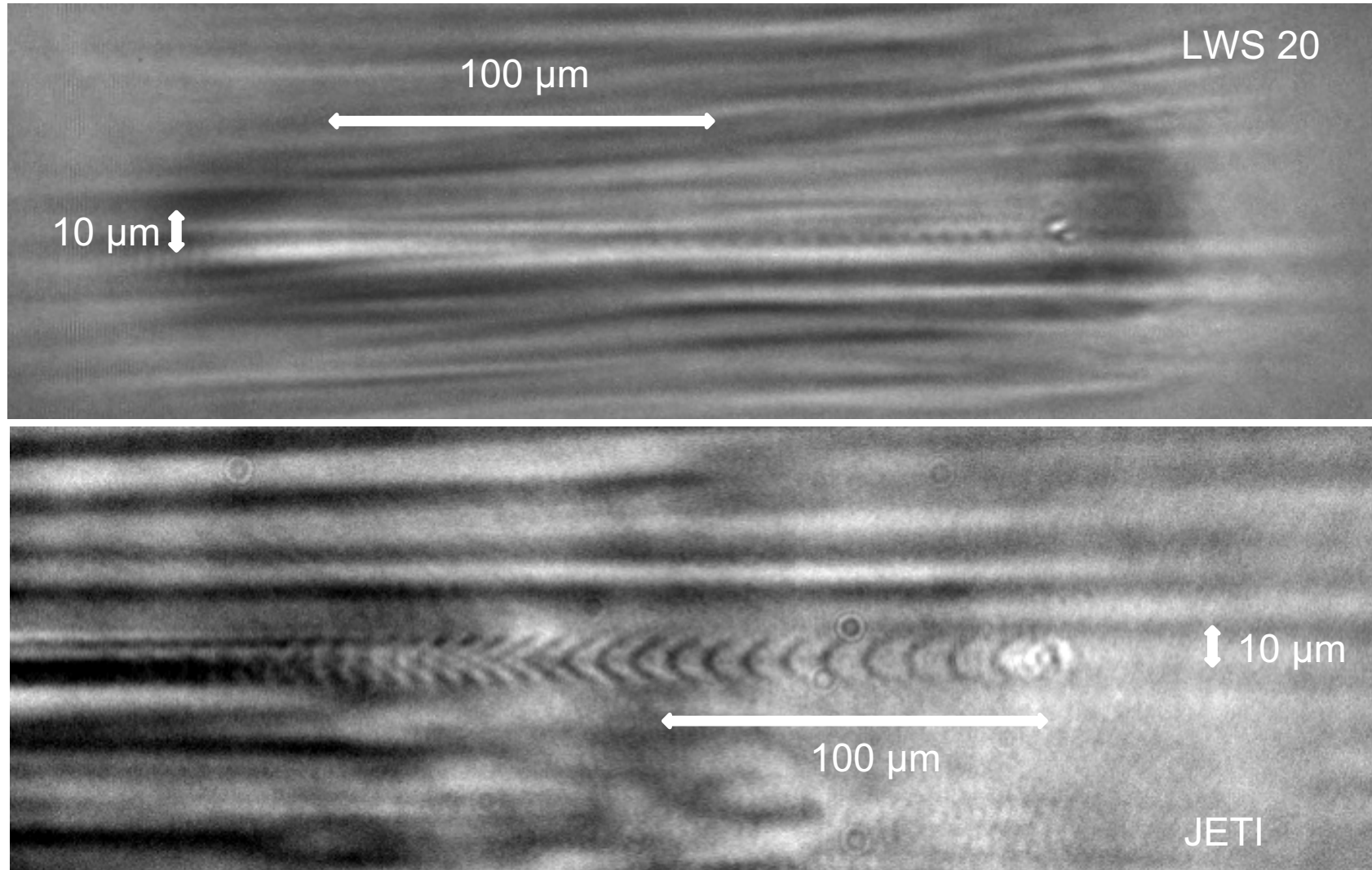
M. Schwab *et al.*, Applied Physics Letters **103**, 191118 (2013)  
 D. Adolph *et al.*, Applied Physics Letters **110**, 081105 (2017)



# Electromagnetic Probe Pulses

## Probing of plasma wakefield acceleration process

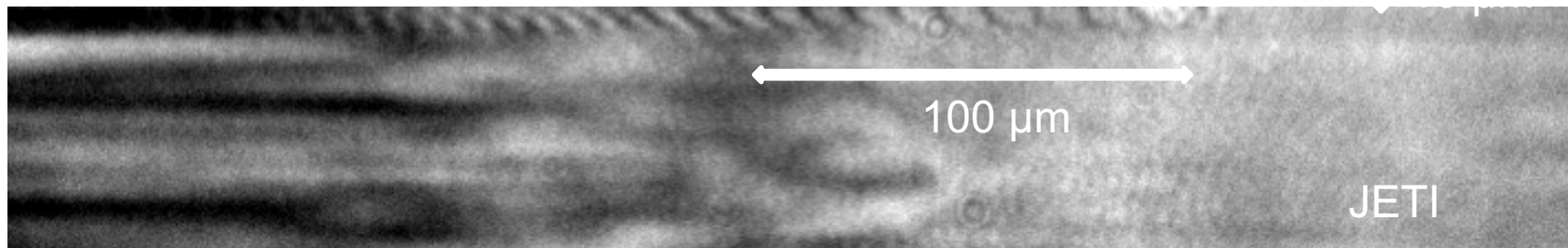
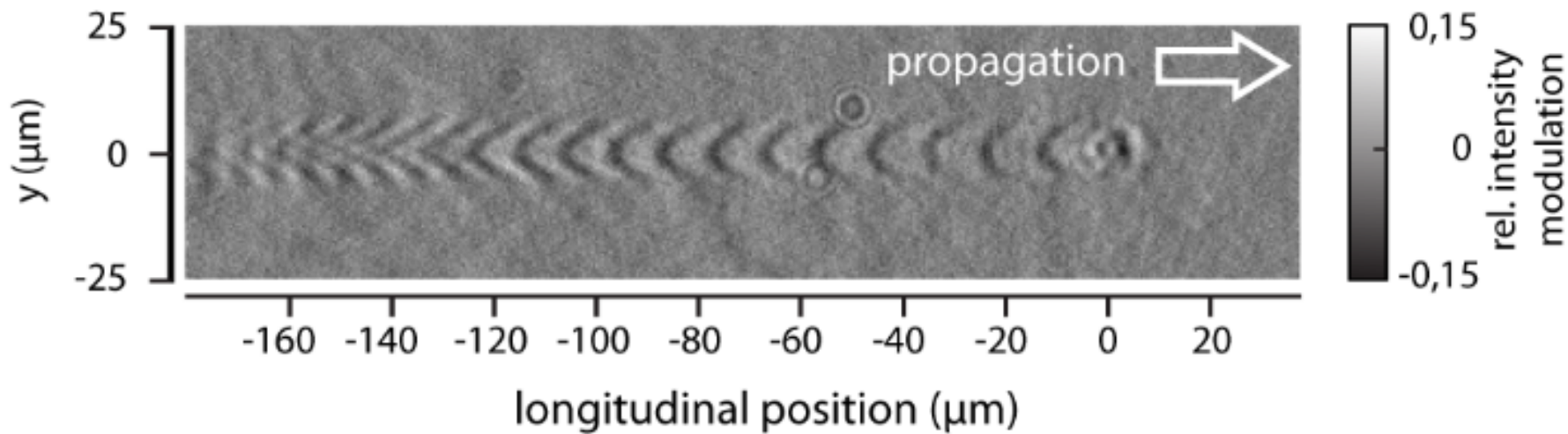
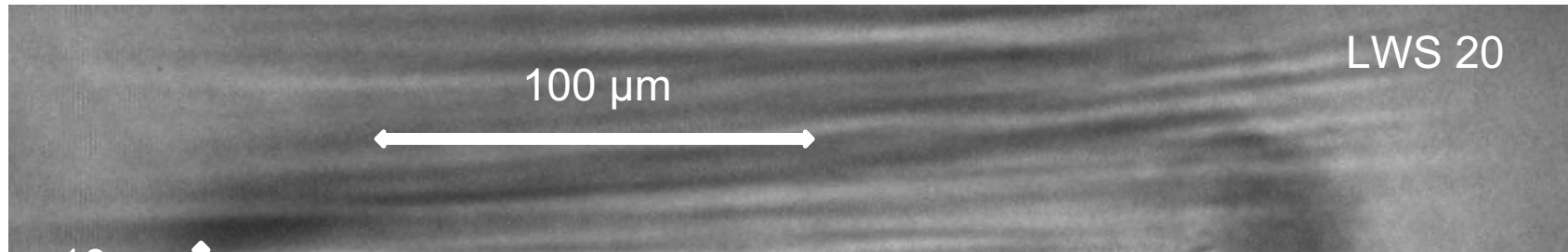
- Few-cycle probe pulses



# Electromagnetic Probe Pulses

## Probing of plasma wakefield acceleration process

- Few-cycle probe pulses



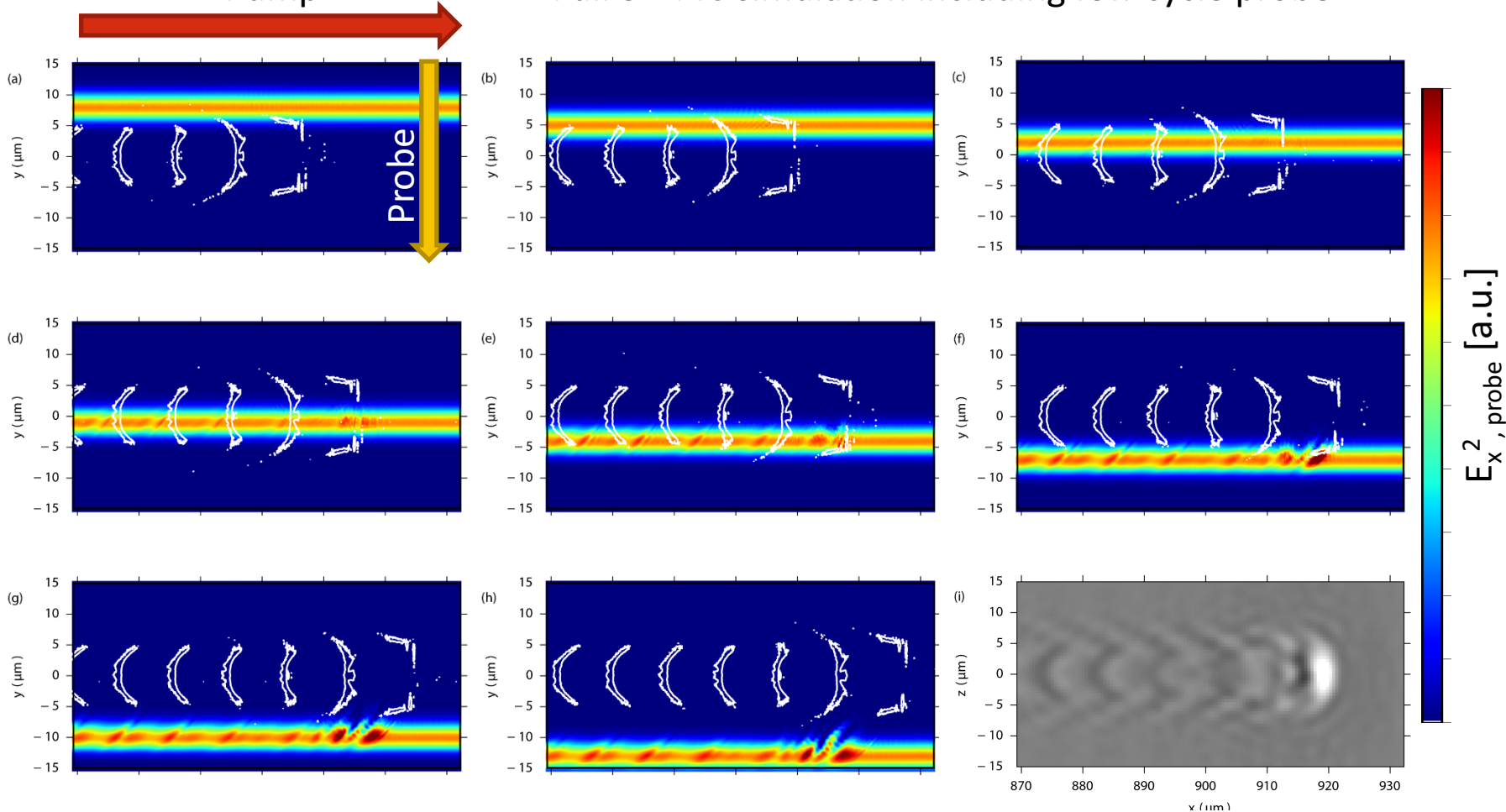


# Electromagnetic Probe Pulses

Probing of plasma wakefield acceleration process

Pump

Full 3D PIC simulation including few cycle probe



Shadowgram is formed mostly in the **center** part.  
High gradients & short pulse duration -> high contrast

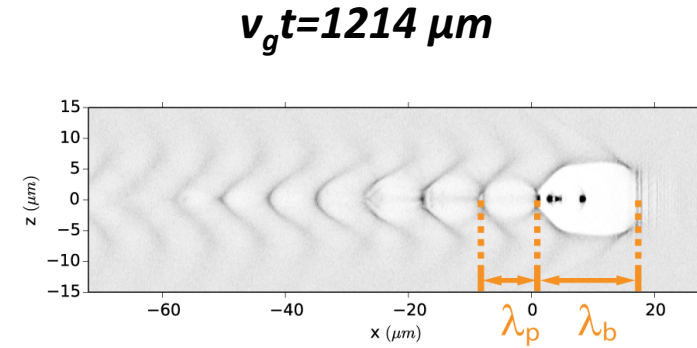
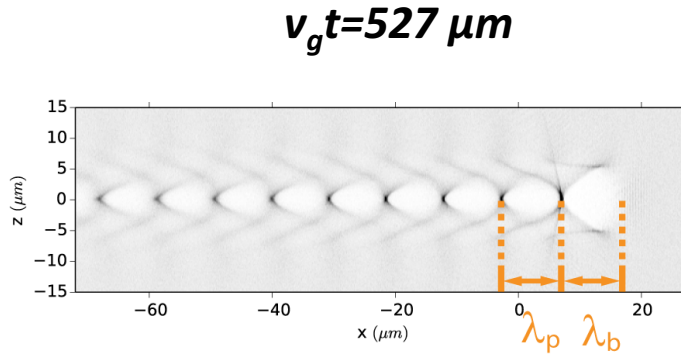
Simulated shadowgram incl. imaging optics and detector



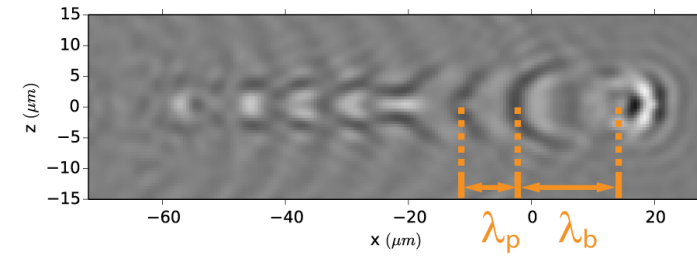
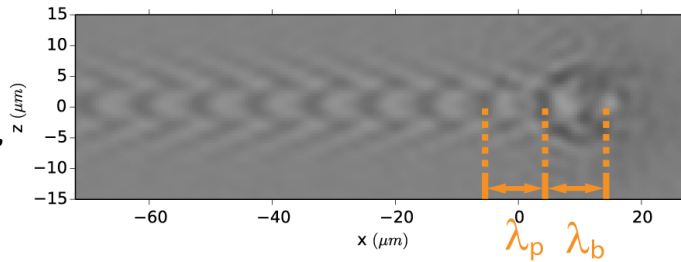
# Electromagnetic Probe Pulses

## Probing of plasma wakefield acceleration process

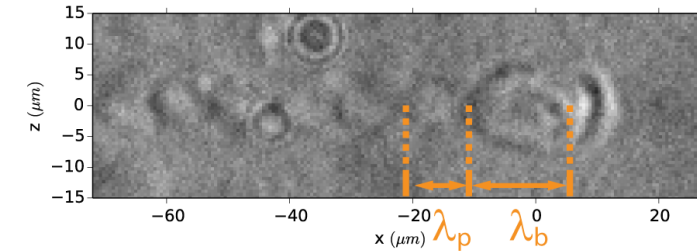
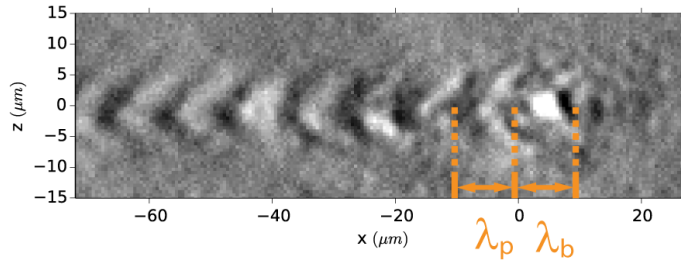
**electron density:**



**computed shadowgram:**



**experiment:**



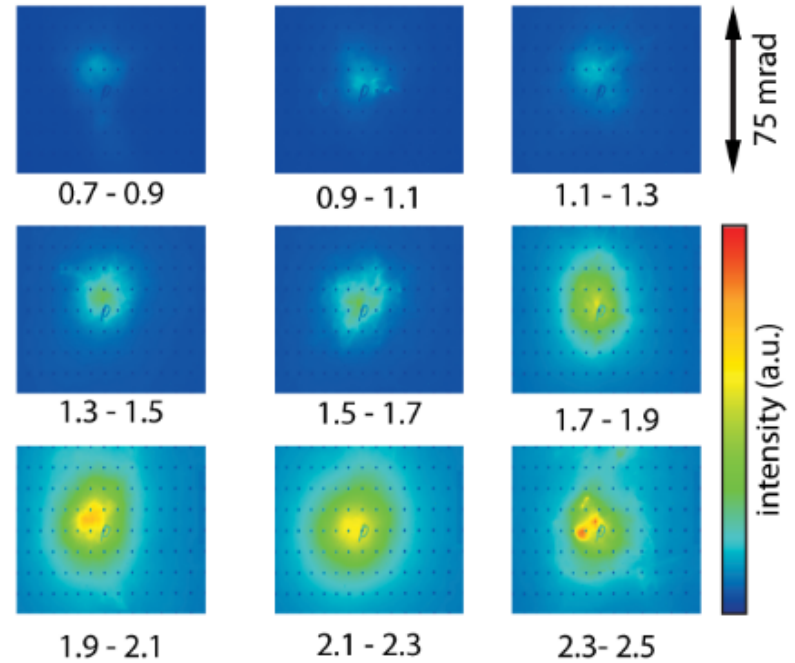
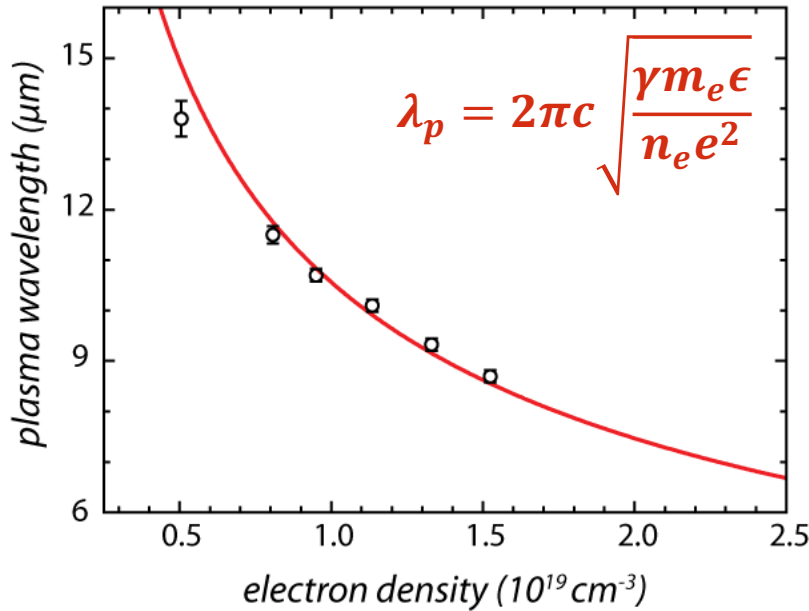
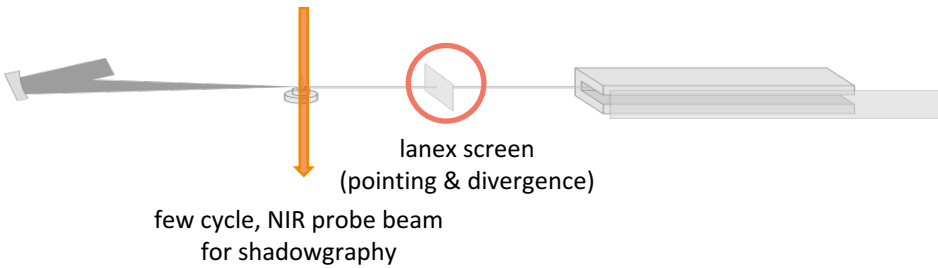
Bubble length and plasma period length are **directly** accessible!





# Electromagnetic Probe Pulses

## Probing of plasma wakefield acceleration process



electron density ( $10^{19} \text{cm}^{-3}$ )

critical power for self trapping:

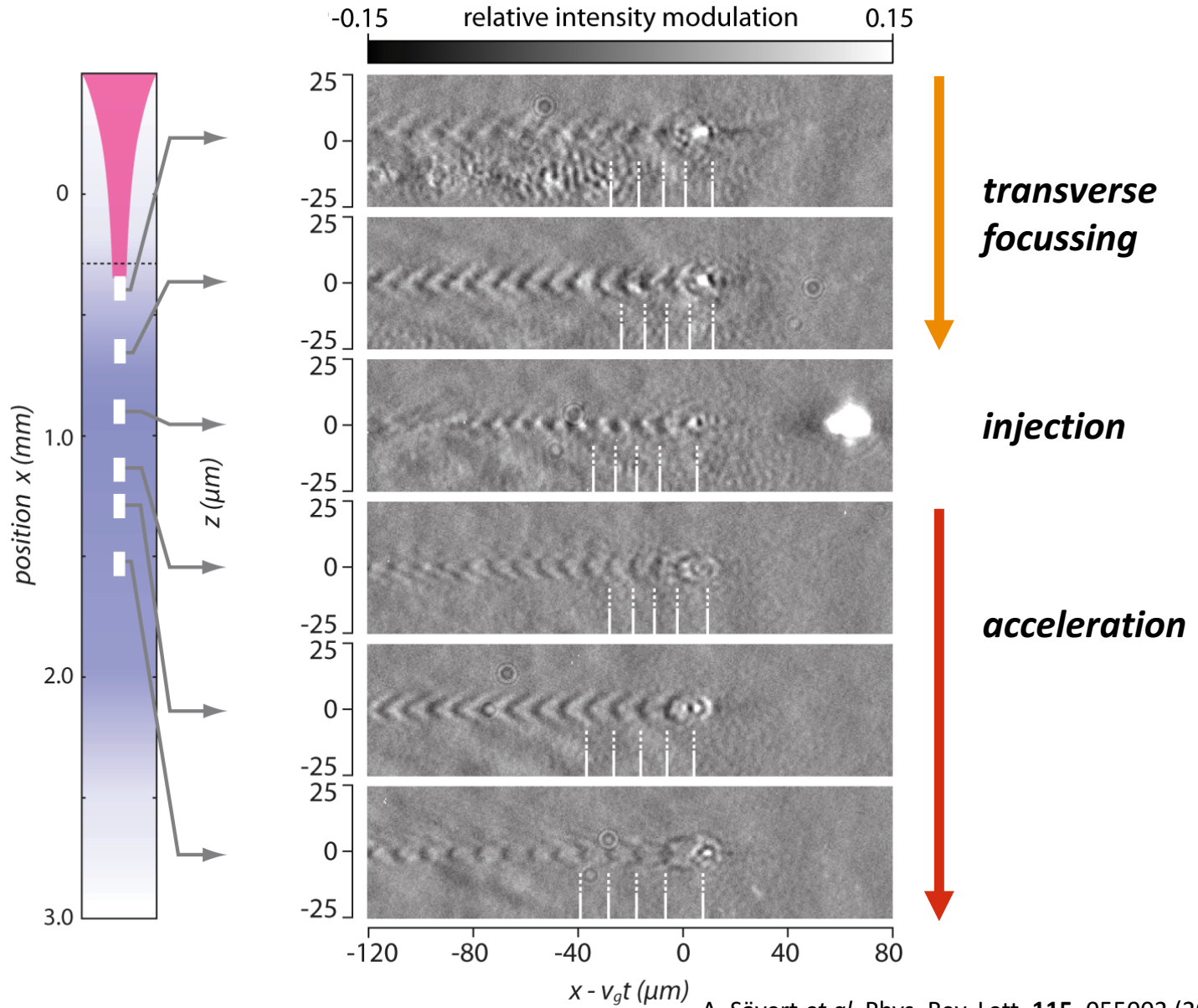
$$\frac{\alpha P}{P_c} > \frac{1}{16} \left[ \ln\left(\frac{2n_c}{3n_e}\right) - 1 \right]^3$$

for our parameters:  $n_e > 1.5 \times 10^{19} \text{cm}^{-3}$



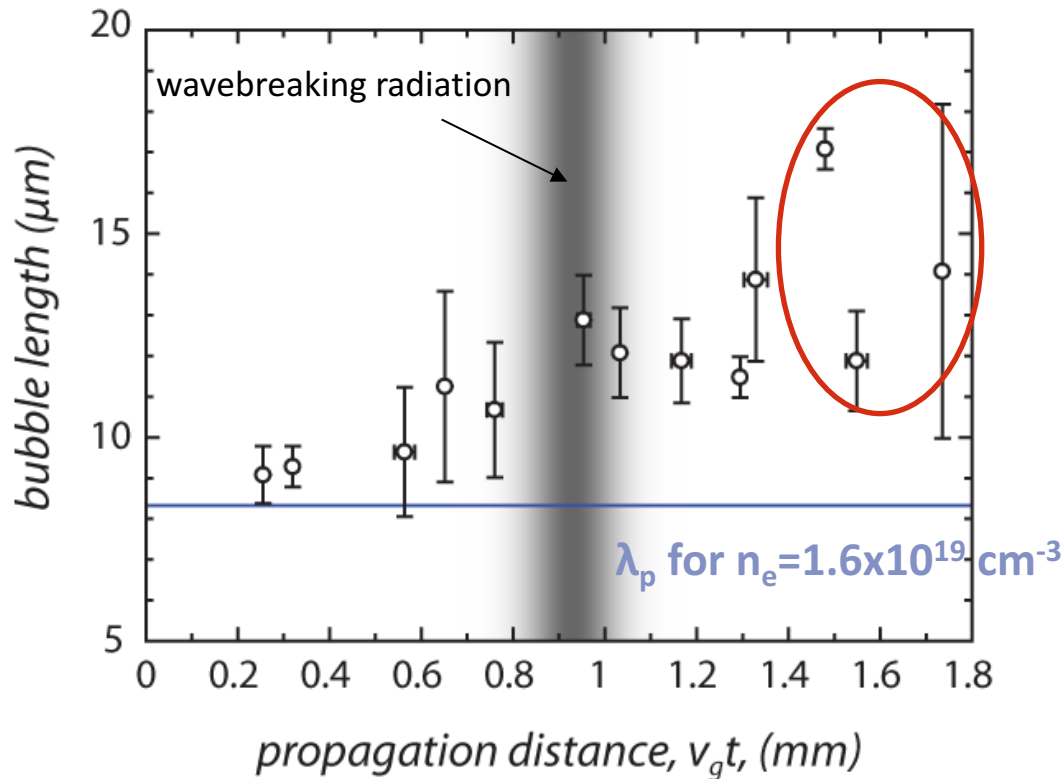
# Electromagnetic Probe Pulses

## Probing of plasma wakefield acceleration process

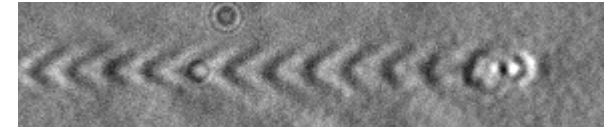


# Electromagnetic Probe Pulses

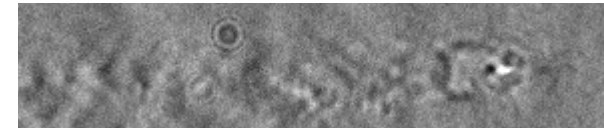
## Probing of plasma wakefield acceleration process



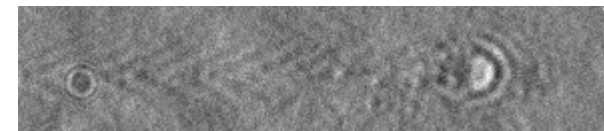
„well behaved“



beam loading dominated



single bubble regime



multiple bubble regime



Bubble expansion starts **before** injection.



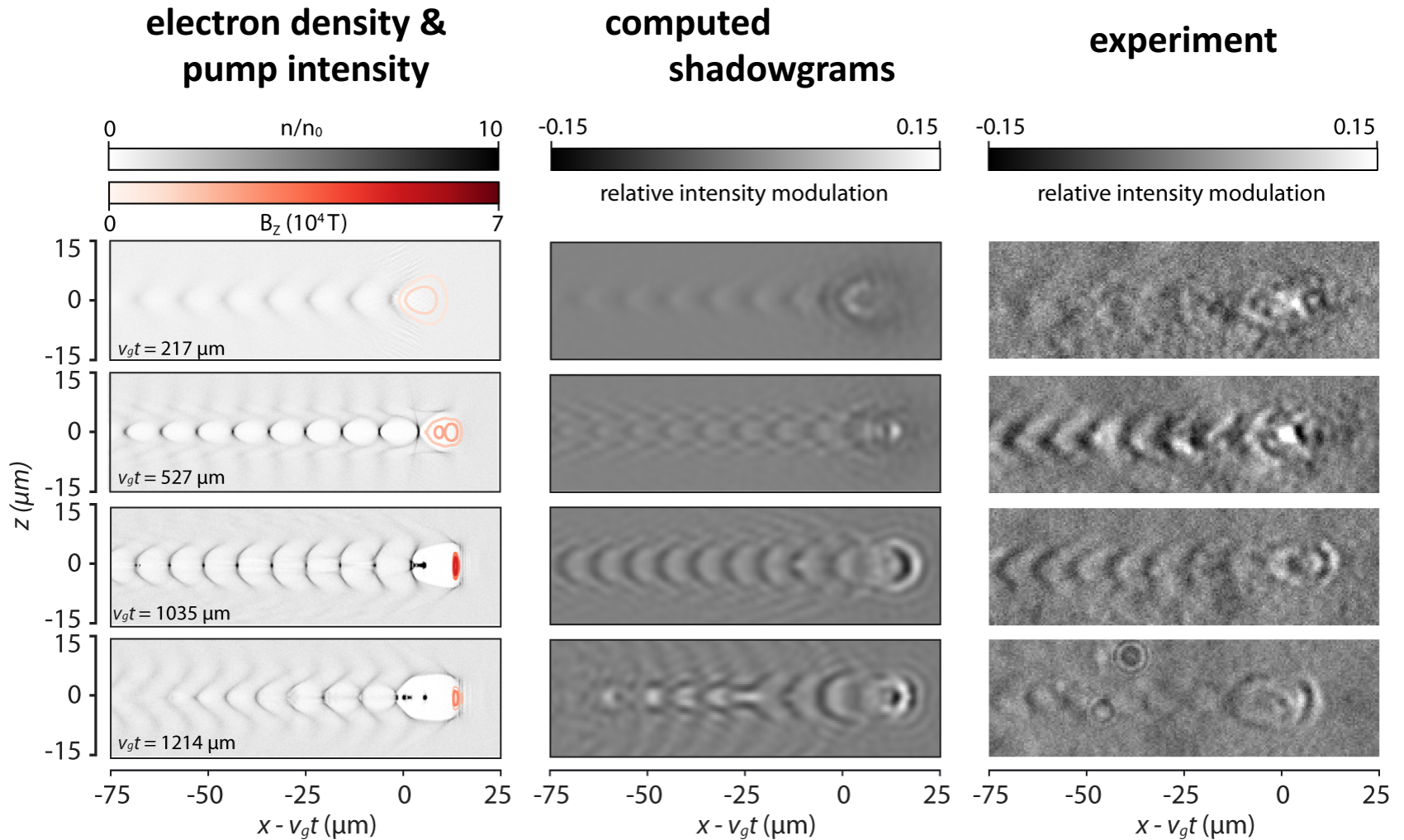
**No beamloading** but amplification of the pump pulse.

$$\lambda_p^* \approx \lambda_p \left( 1 + \frac{\alpha_0^2}{2} \right)^{1/4}$$



# Electromagnetic Probe Pulses

## Probing of plasma wakefield acceleration process

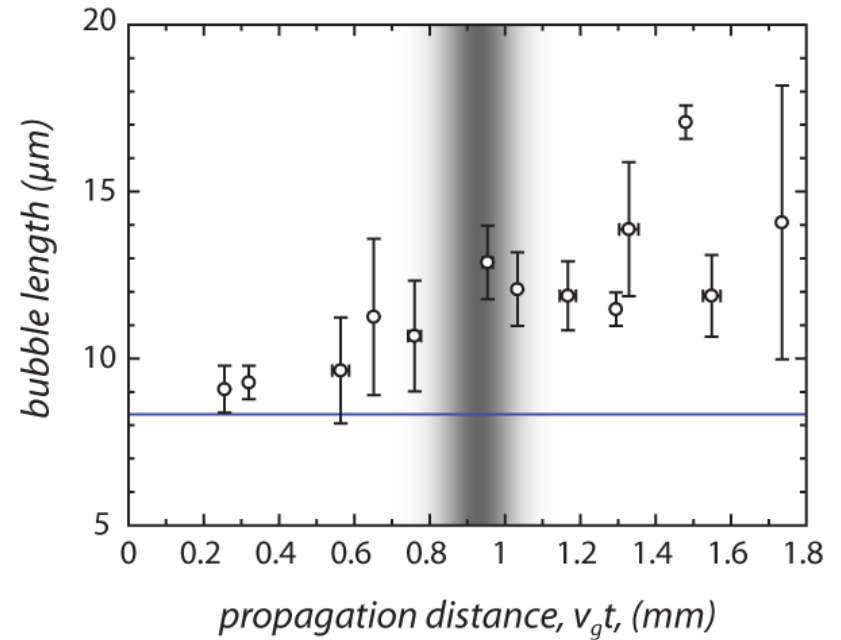
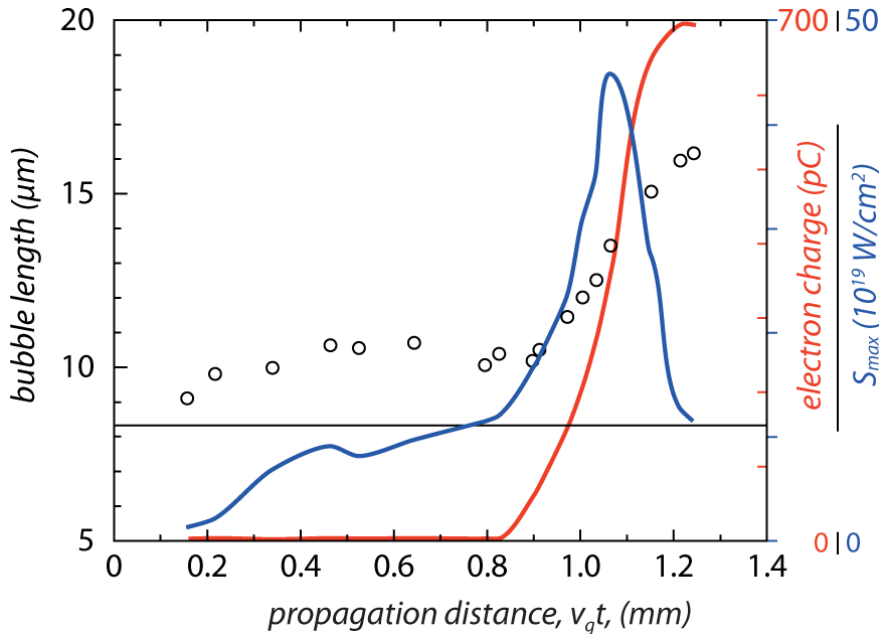


3D PIC simulation (EPOCH),  $150 \times 70 \times 70 \mu\text{m}^3$  sliding box  
2700x525x525 cells



# Electromagnetic Probe Pulses

## Probing of plasma wakefield acceleration process



Bubble expansion starts **before** injection.



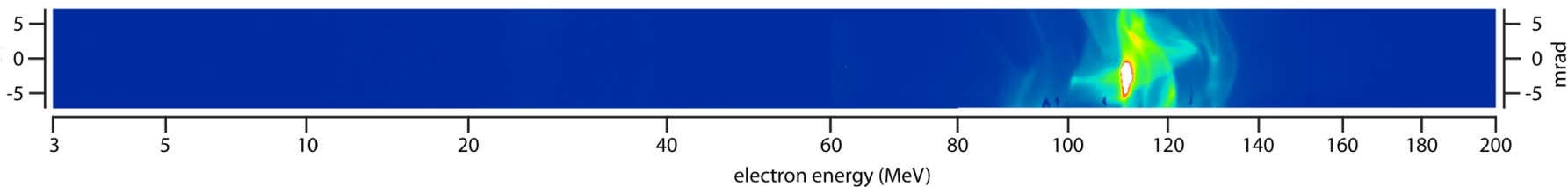
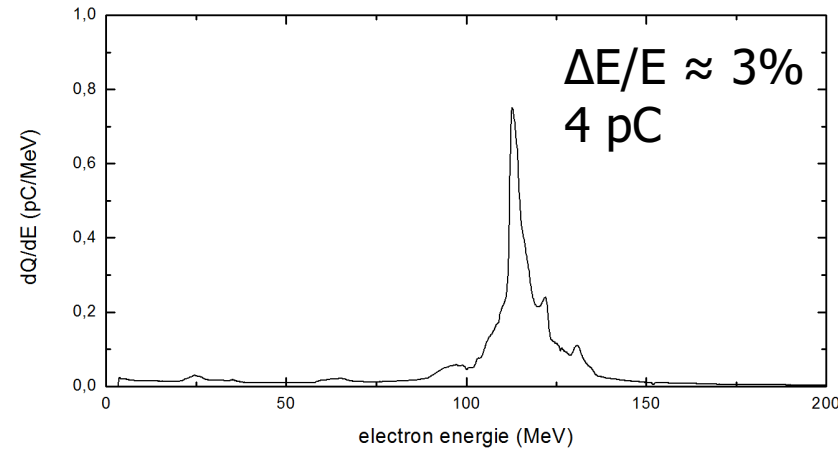
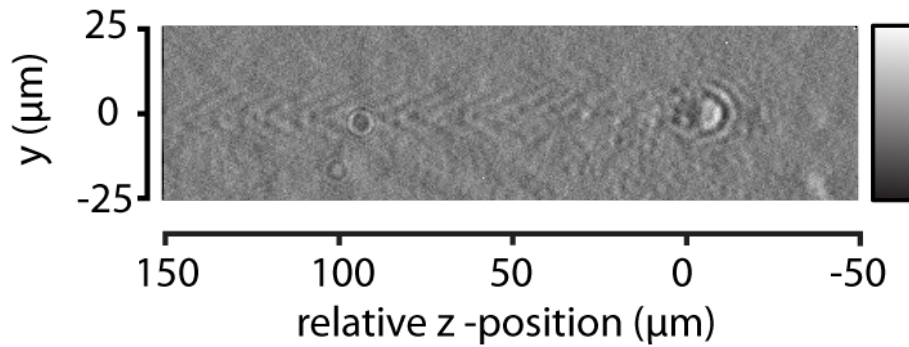
**No beamloading** but amplification of the pump pulse.



# Electromagnetic Probe Pulses

## Probing of plasma wakefield acceleration process

- After plasma wave evolution into single bubble:





# Electromagnetic Probe Pulses

## Probing of plasma wakefield acceleration process

Energy gain

$$\Delta E [GeV] \cong 1.7 \left( \frac{P [TW]}{100} \right)^{1/3} \left( \frac{10^{18}}{n_p [cm^{-3}]} \right)^{2/3} \left( \frac{0.8}{\lambda_0 [\mu m]} \right)^{4/3}$$

W. Lu et al. Phys. Rev. ST Accel. Beams 10, 061301

lower plasma density



lower plasma frequency

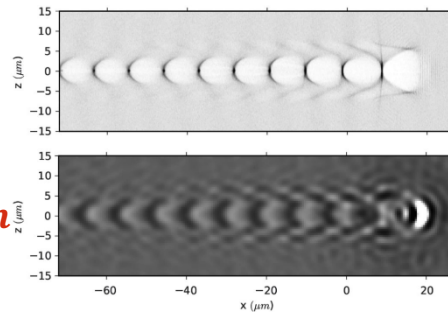
**JETi 200:**  $P = 200 \text{ TW}$ ,  
 $\tau_L = 17 \text{ fs}$   
pulse duration:  $\tau_L \leq \lambda_p / 2$

$$\lambda_p = 750 \text{ nm}$$

$$\lambda_p = 1.4 \mu m$$

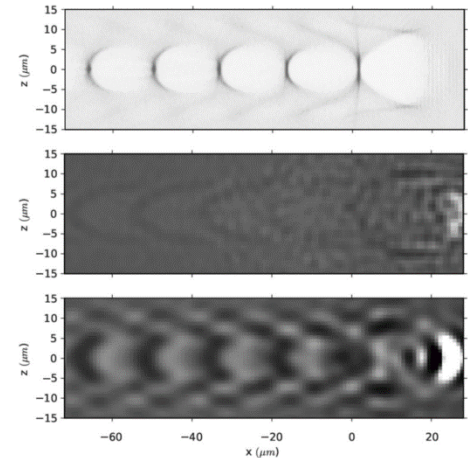
**JETi40**

$$n_p = 1.6 \times 10^{19} \text{ cm}^{-3}$$



**JETi200**

$$n_p = 0.4 \times 10^{19} \text{ cm}^{-3}$$



For probing techniques, the refractive index

$$n = \sqrt{1 - \frac{\omega_p^2}{\gamma \omega_{probe}^2}}$$

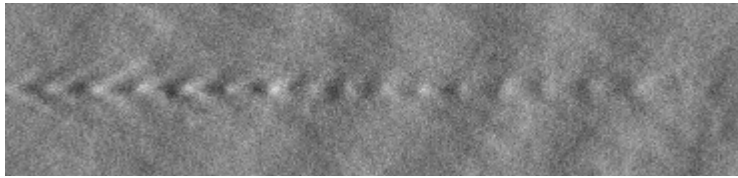
defines the sensitivity!



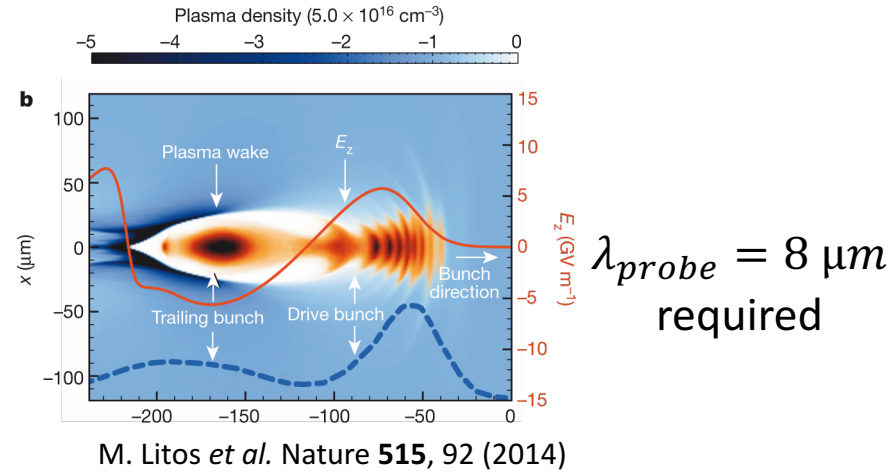
# Electromagnetic Probe Pulses

## Probing of plasma wakefield acceleration process

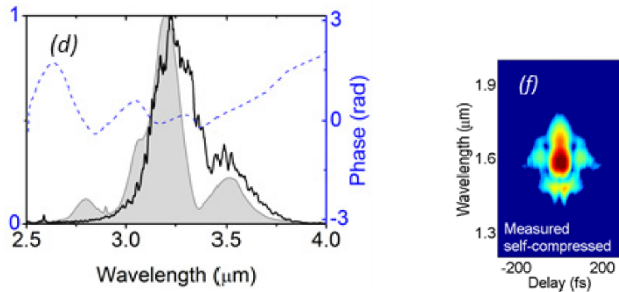
$$n_e = 7 \cdot 10^{18} \text{ cm}^{-3}, \lambda_p = 12 \mu\text{m}$$



$$\lambda_{probe} = 750 \text{ nm}$$



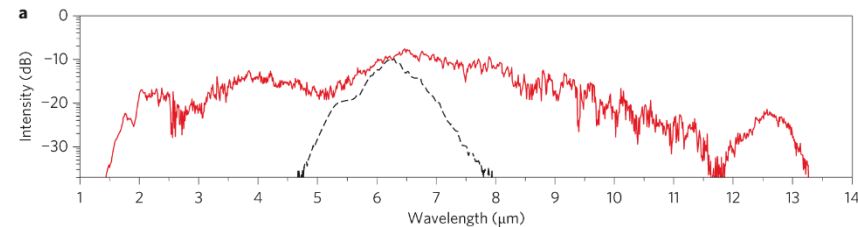
### Sub 3-cycle laser pulses @ $\lambda_c = 3.1 \mu\text{m}$



$$E_{pulse} = 10 \mu\text{J} @ 160 \text{ kHz}$$

M. Hemmer *et al.* Optics Express **21**, 28095 (2013)

### Super continuum @ $\lambda_c = 6.5 \mu\text{m}$



$$E_{pulse} = 100 \text{ nJ} @ 1 \text{ kHz}$$

C.R. Petersen *et al.* Nat. Photon. **8**, 830 (2014)



All optical techniques like shadowgraphy (imaging wakefields), polarimetry (imaging magnetic fields) are feasible for PWFA experiments!





# Electromagnetic Probe Pulses

## Probing of laser-driven ion acceleration process

### TNSA (Target Normal Sheath Acceleration)

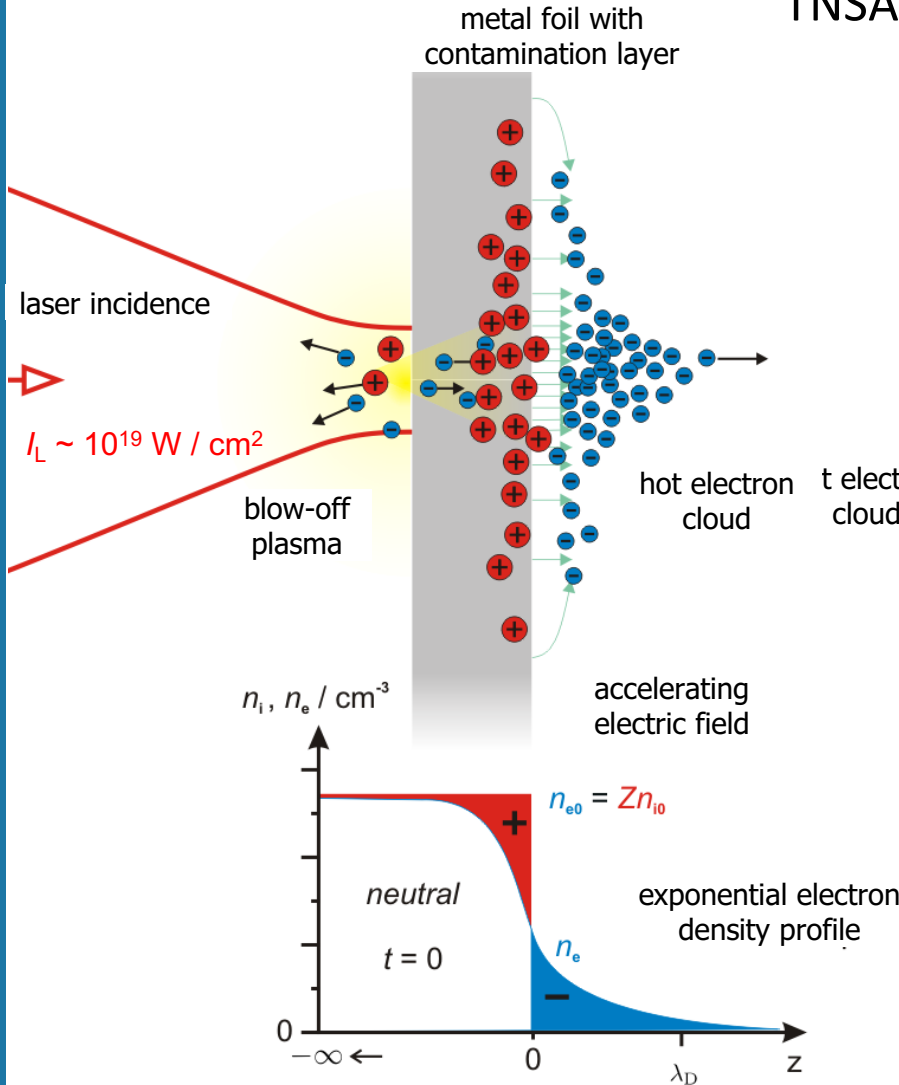
- laser pulse generates relativistic electrons,
- they propagate through the foil and
- form an electric sheath field

$$\sim \text{TV/m} \quad \mathcal{E}_{\text{front}}(t) \approx 2 \sqrt{\frac{k_B T_e n_e}{\epsilon_0 (2e_N + \omega_{pi}^2 t^2)}}$$

- charge distribution starts to expand,
- acceleration length  $\sim \mu\text{m}$
- $\sim$  Debye-length  $\lambda_D = \sqrt{\frac{\epsilon_0 k_B T_e}{n_e e^2}}$
- lifetime of electric field  $\sim f(\tau_L)$
- max. ion energies

$$E_{\text{max}} = 2Zk_B T_e \left[ \ln \left( \frac{\omega_{pi} t}{\sqrt{2} e_N} + \sqrt{\left( \frac{\omega_{pi} t}{\sqrt{2} e_N} \right)^2 + 1} \right) \right]^2$$

P. Mora, PRL **90**, 185002 (2003)





# Electromagnetic Probe Pulses

## Probing of laser-driven ion acceleration process

### TNSA (Target Normal Sheath Acceleration)

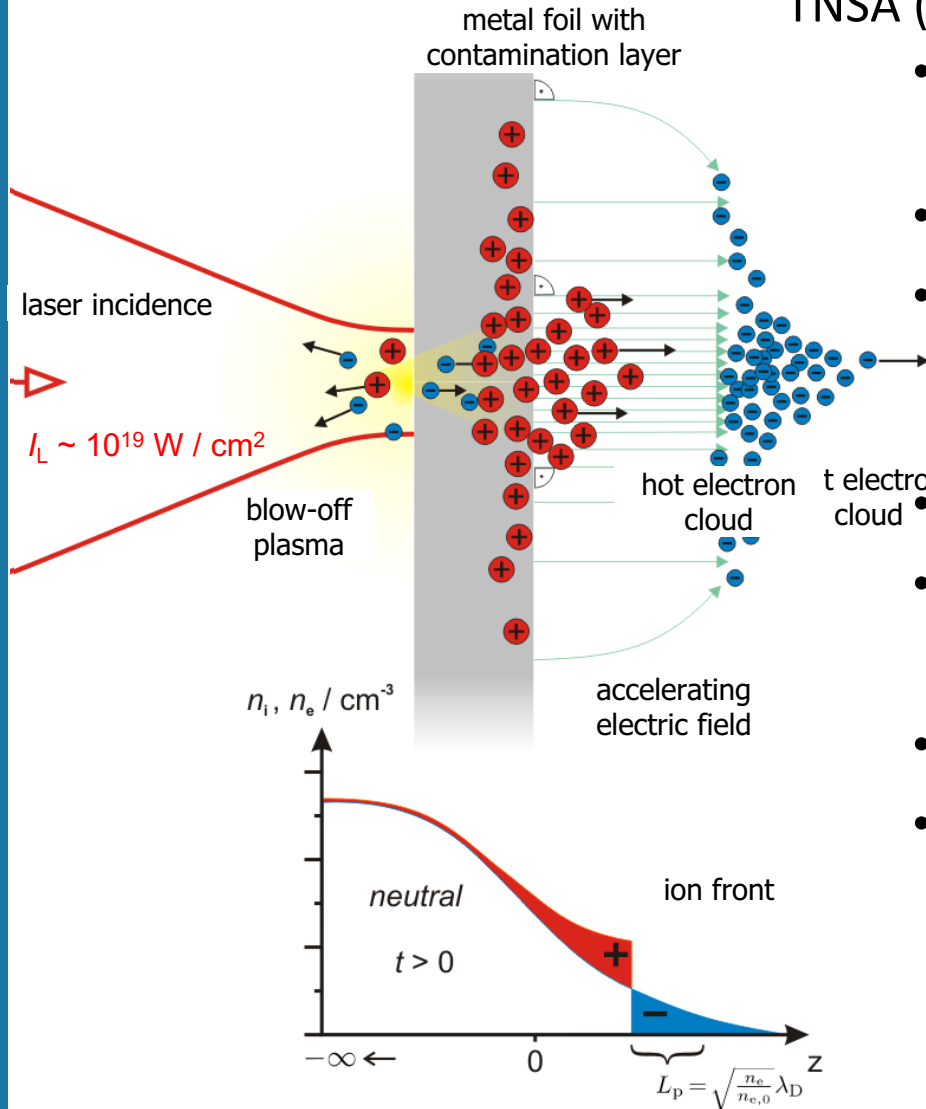
- laser pulse generates relativistic electrons,
- they propagate through the foil and
- form an electric sheath field

$$\sim \text{TV/m} \quad E_{\text{front}}(t) \approx 2 \sqrt{\frac{k_B T_e n_e}{\epsilon_0 (2e_N + \omega_{pi}^2 t^2)}}$$

- charge distribution starts to expand,
- acceleration length  $\sim \mu\text{m}$
- $\sim$  Debye-length  $\lambda_D = \sqrt{\frac{\epsilon_0 k_B T_e}{n_e e^2}}$
- lifetime of electric field  $\sim f(\tau_L)$
- max. ion energies

$$E_{\text{max}} = 2Z k_B T_e \left[ \ln \left( \frac{\omega_{pi} t}{\sqrt{2e_N}} + \sqrt{\left( \frac{\omega_{pi} t}{\sqrt{2e_N}} \right)^2 + 1} \right) \right]^2$$

P. Mora, PRL **90**, 185002 (2003)

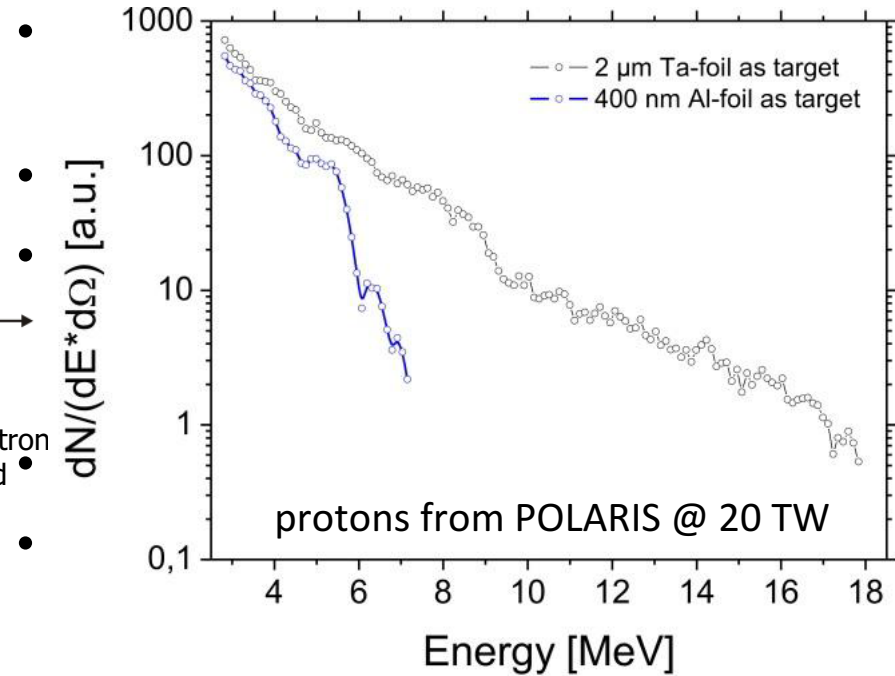
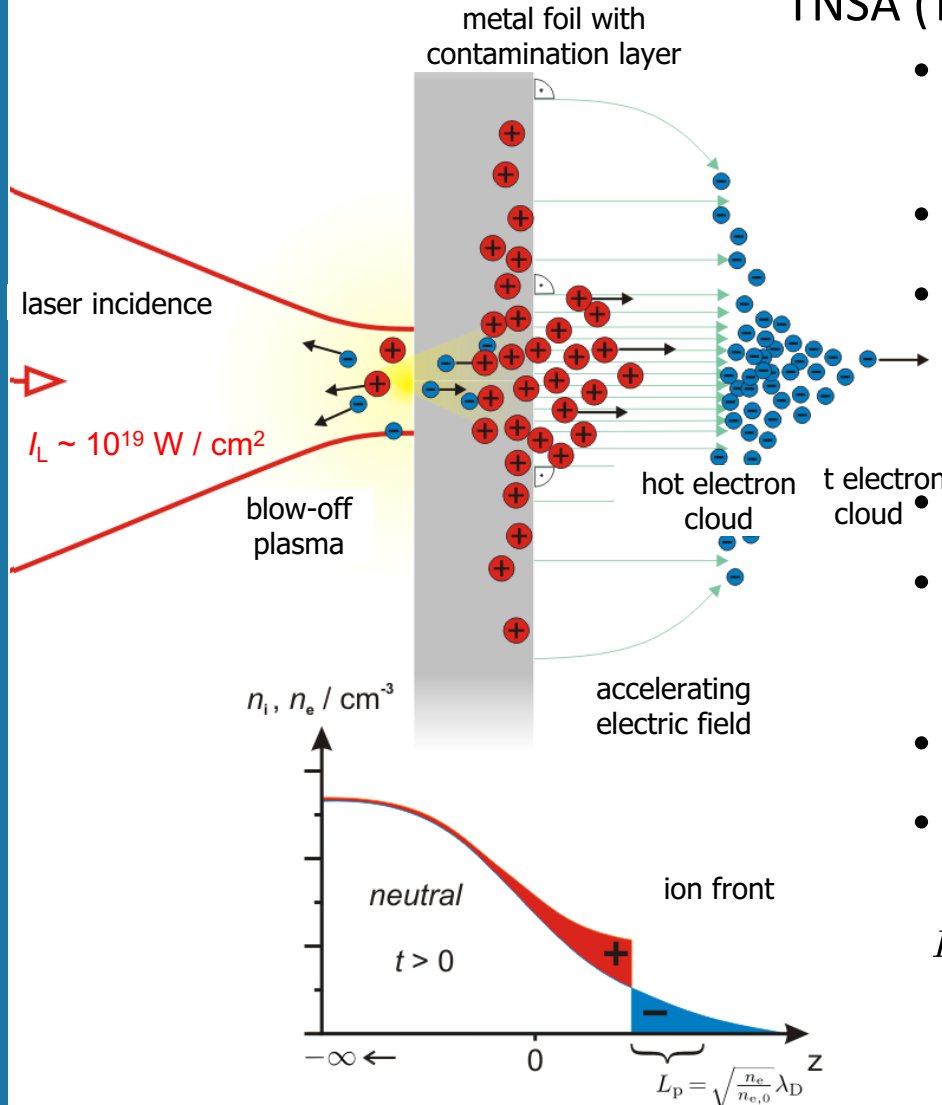




# Electromagnetic Probe Pulses

## Probing of laser-driven ion acceleration process

### TNSA (Target Normal Sheath Acceleration)



- lifetime of electric field  $\sim f(\tau_L)$
- max. ion energies

$$E_{\max} = 2Zk_B T_e \left[ \ln \left( \frac{\omega_{pi} t}{\sqrt{2} e_N} + \sqrt{\left( \frac{\omega_{pi} t}{\sqrt{2} e_N} \right)^2 + 1} \right) \right]^2$$

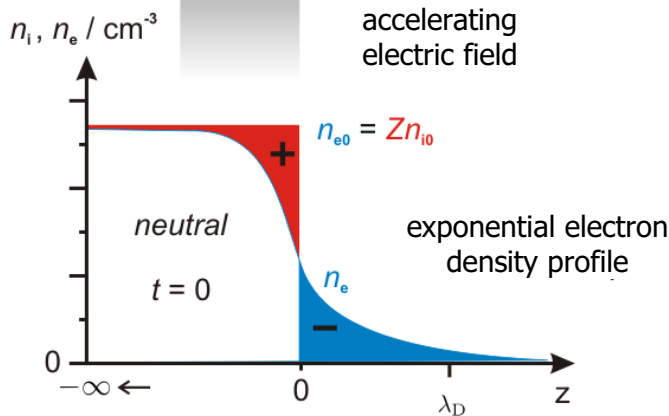
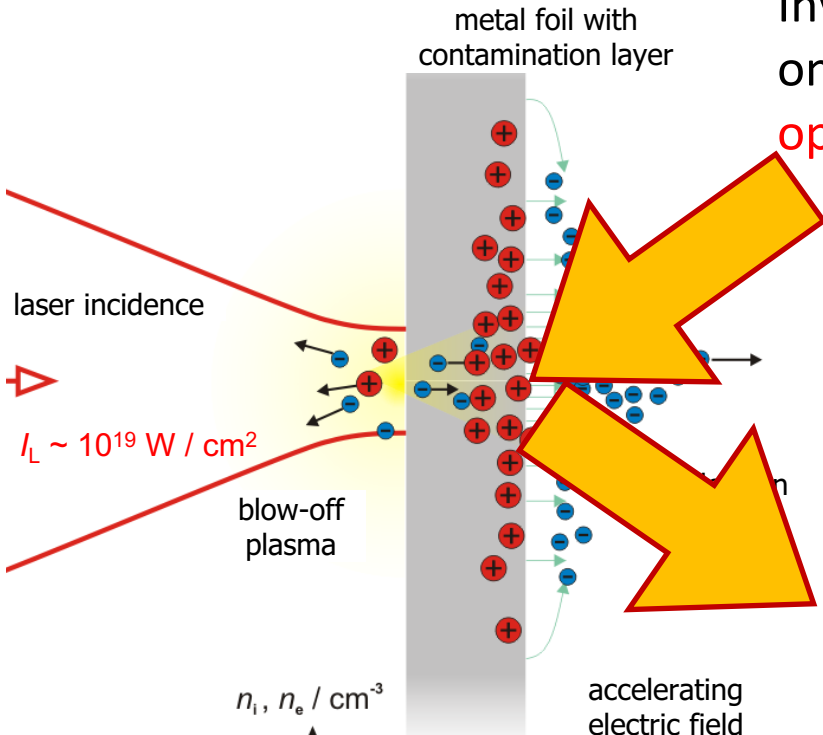
P. Mora, PRL **90**, 185002 (2003)



# Electromagnetic Probe Pulses

## Probing of laser-driven ion acceleration process

Investigation of rear-surface TNSA-sheath at onset of acceleration process:  
**optical probing with fs and  $\mu\text{m}$  resolution**

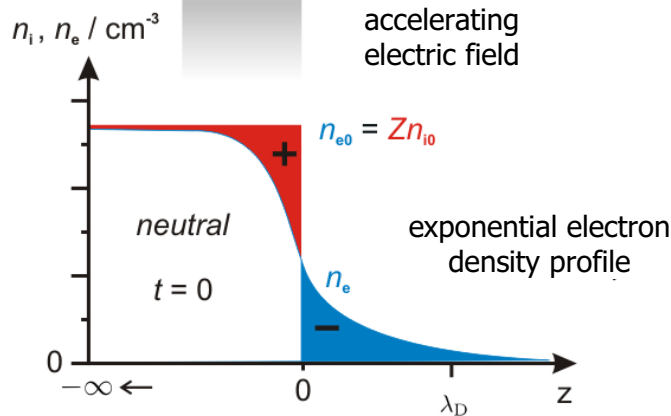
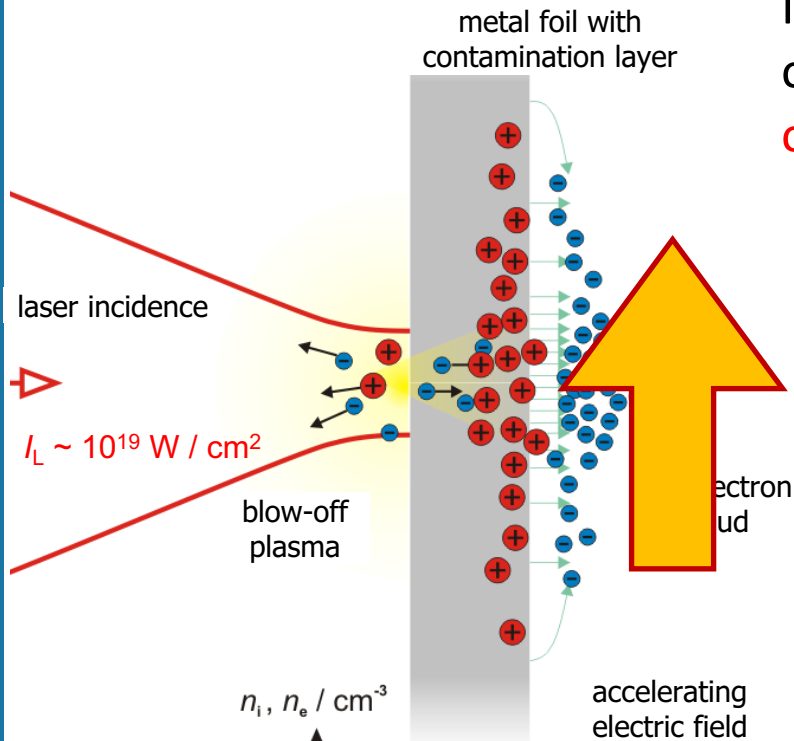




# Electromagnetic Probe Pulses

## Probing of laser-driven ion acceleration process

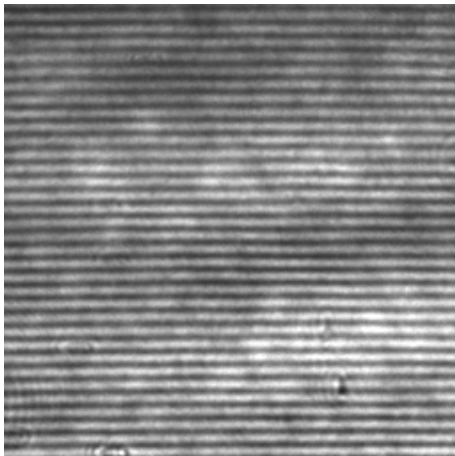
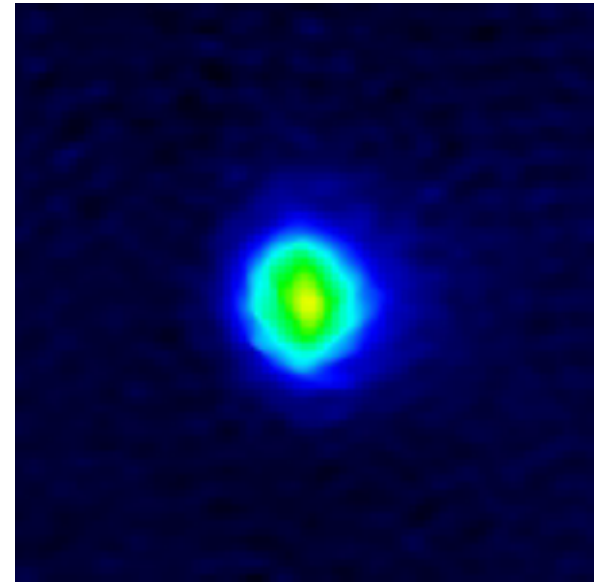
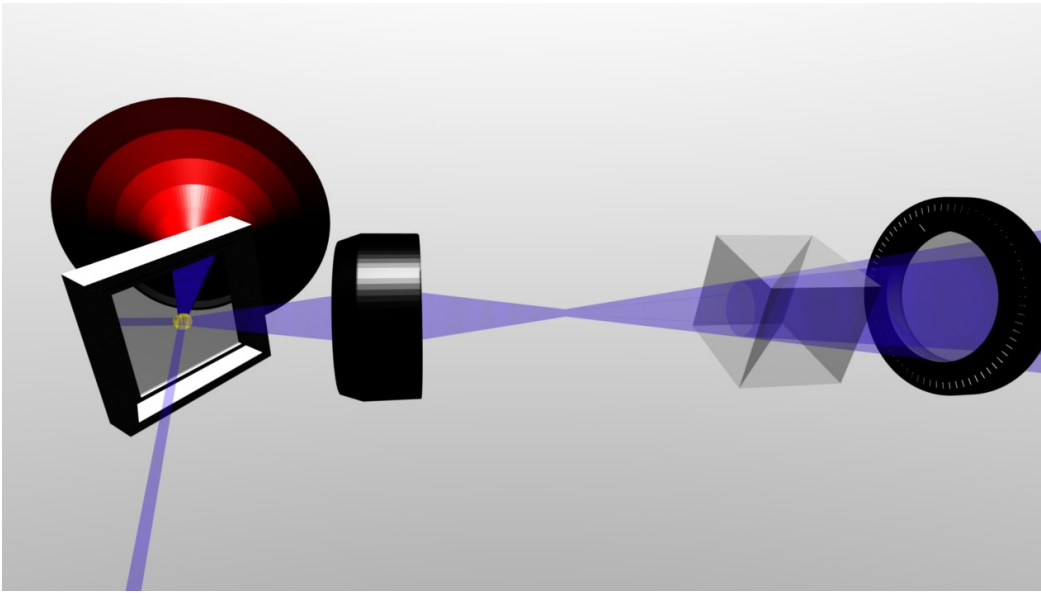
Investigation of rear-surface TNSA-sheath at onset of acceleration process:  
**optical probing with fs and  $\mu\text{m}$  resolution**



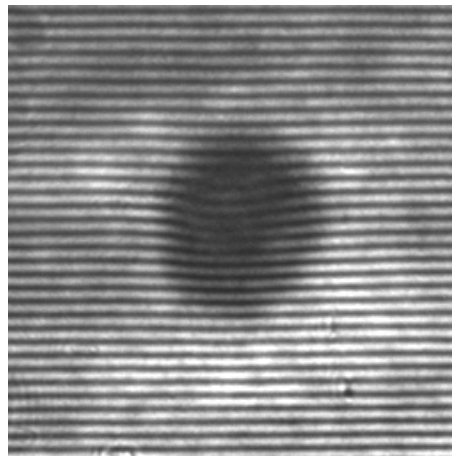


# Electromagnetic Probe Pulses

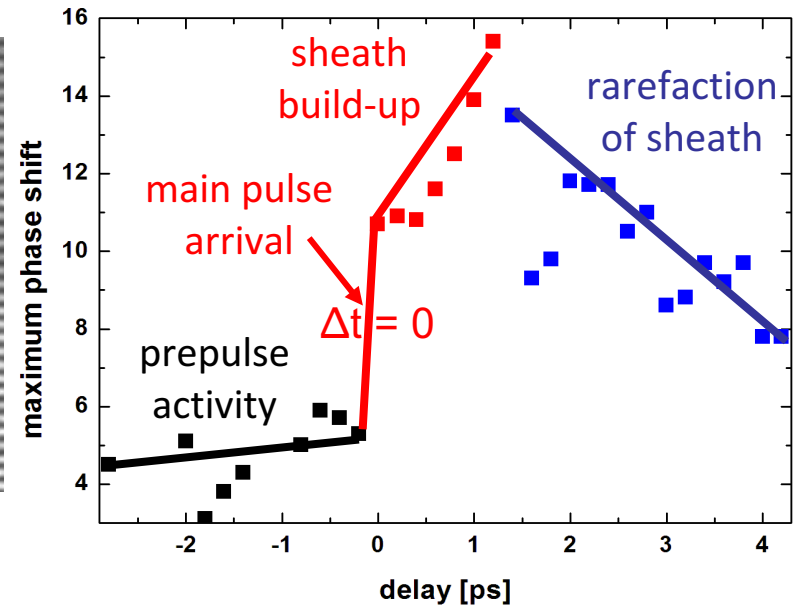
## Probing of laser-driven ion acceleration process



without main pulse



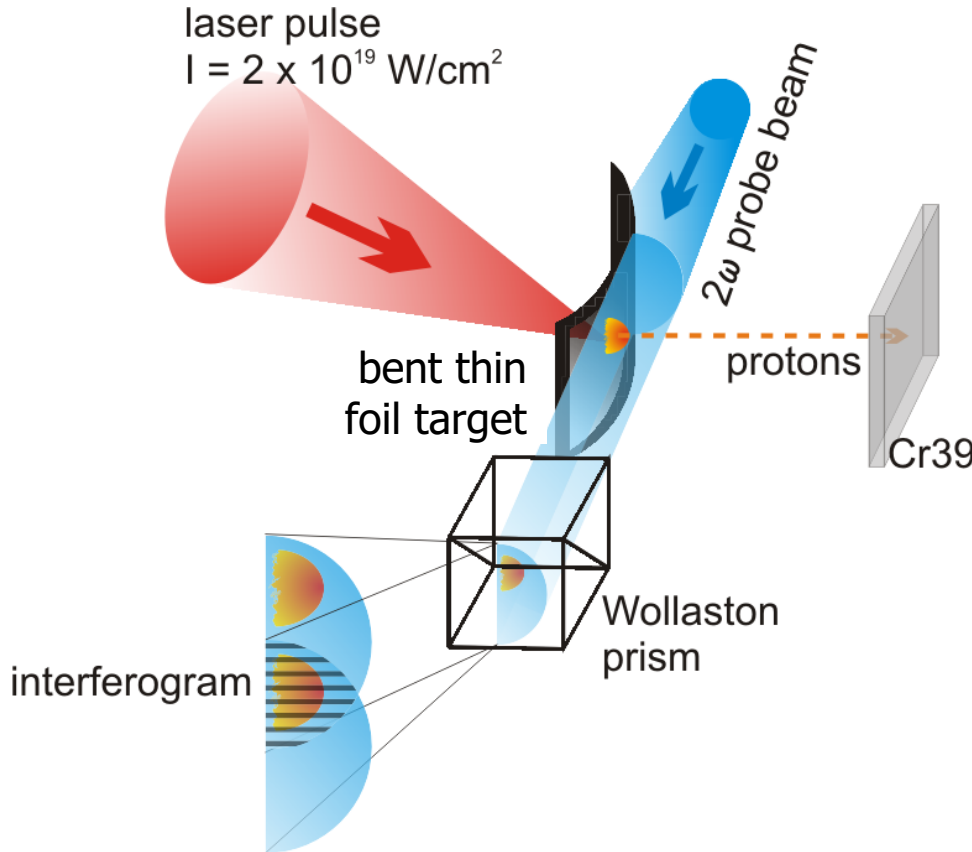
with main pulse





# Electromagnetic Probe Pulses

## Probing of laser-driven ion acceleration process



phase shift (measured tangentially)  $\Rightarrow$  2D signal

$$\Delta\phi = \frac{\omega}{c} \int (\eta - 1) ds = \frac{\omega}{c} \int \left( \sqrt{1 - \frac{n_e}{n_c}} - 1 \right) ds$$

$$\approx \frac{\omega}{2cn_c} \int n_e ds$$

Abel inversion

$$h(y) = 2 \int_y^R f(y) \frac{r}{\sqrt{r^2 - y^2}} dr$$

3D electron density distribution (cylindrical symmetry)

$$n_e(r, z, t) \sim \exp \left[ -\frac{r(t)^2}{w_0^2} \right] \exp \left[ -\frac{z(t)}{\lambda_D} \right]$$

Nomarski interferometer:  
f/2 imaging onto 12-bit CCD  
Wollaston prism + polarizer

- spatial resolution  $\sim 1.1 \mu\text{m}$
  - temporal resolution  $\sim 100 \text{ fs}$
- $\Rightarrow$  match dimensions of acceleration process!

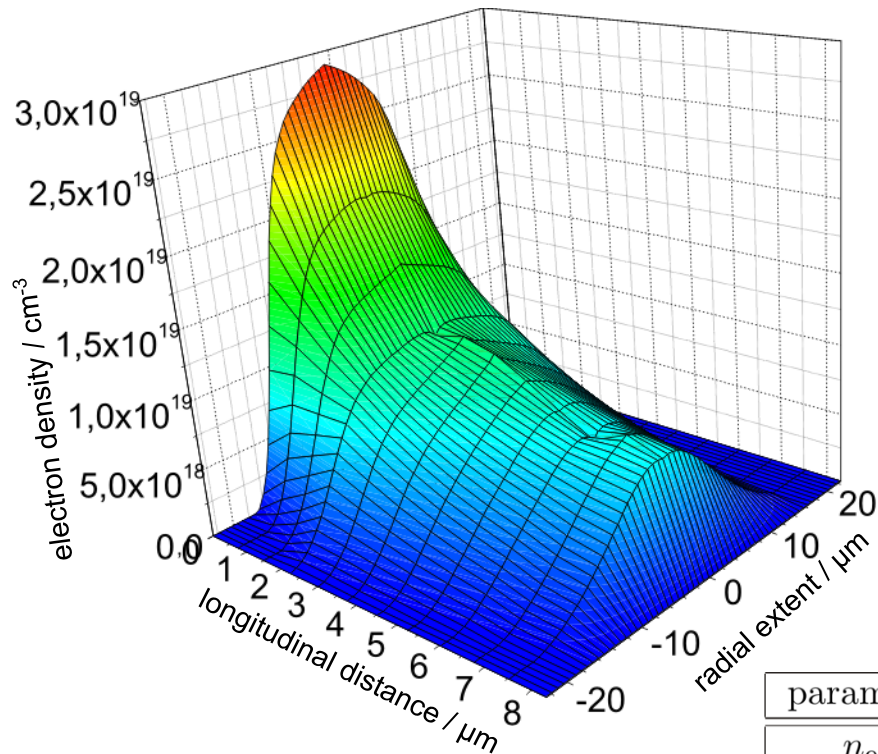
R. Benattar *et al.* (1979); G. Pretzler *et al.* (1992)



# Electromagnetic Probe Pulses

## Probing of laser-driven ion acceleration process

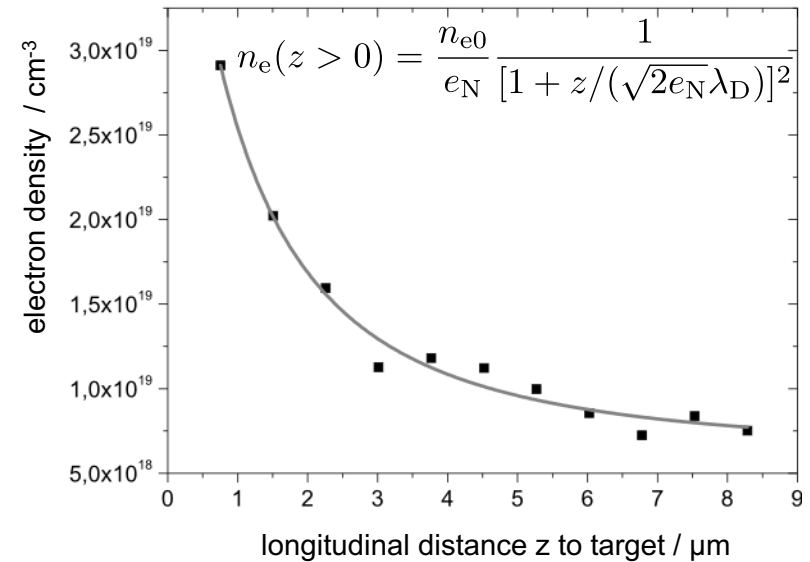
1<sup>st</sup> all-optical measurement of  $n_e$ -distribution driving laser ion acceleration!



at  $t = 0$

(onset of acceleration process)

J. Crow *et al.*, J. Plasma Phys. (1975)



parameter	experimental data	theoretical prediction
$n_{e0}$	$(8.4 \pm 0.4) \times 10^{19} \text{ cm}^{-3}$	$9.44 \times 10^{19} \text{ cm}^{-3}$
$\lambda_D$	$(1.0 \pm 0.2) \mu\text{m}$	$0.64 \mu\text{m}$
$w_{\text{back}}$	$(21 \pm 1) \mu\text{m}$	$8.1 \mu\text{m}$
$k_B T_e$	$(1.5 \pm 0.4) \text{ MeV}$	$0.71 \text{ MeV}$
$E_{\text{TNSA}}$	$(1.3 \pm 0.4) \text{ TV/m}$	$1.1 \text{ TV/m}$

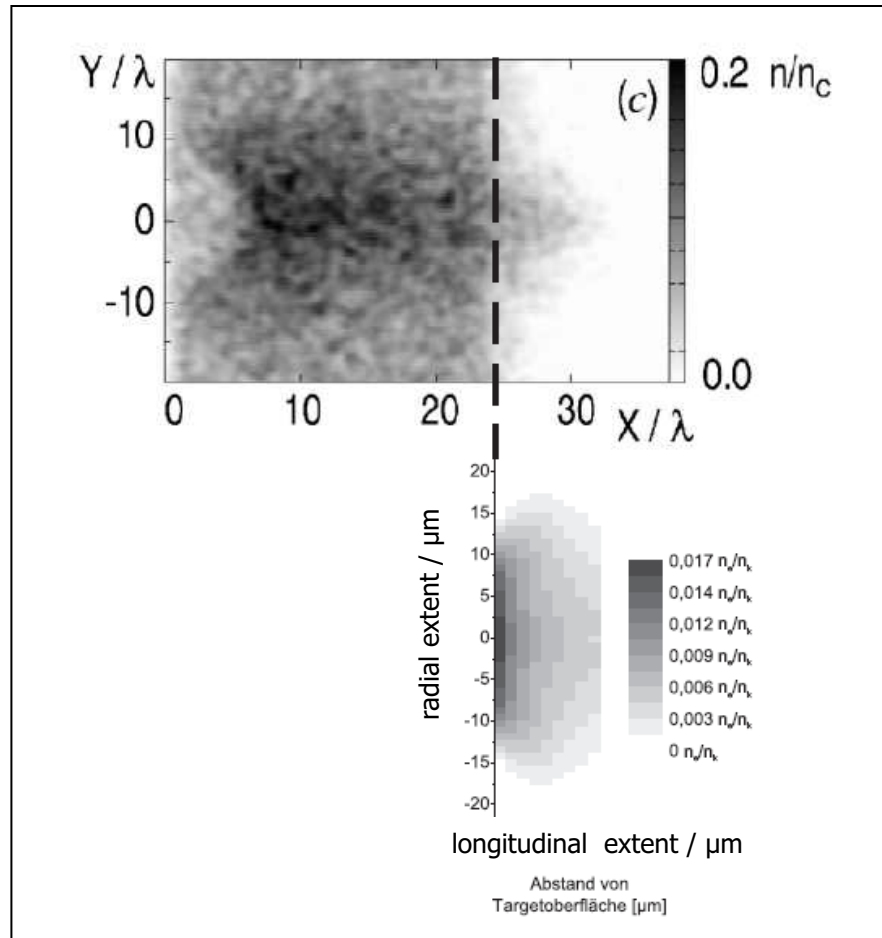
O. Jäckel, MCK *et al.*, New Journal of Physics **12**, 103027 (2010)



# Electromagnetic Probe Pulses

## Probing of laser-driven ion acceleration process

Comparison with numerical simulations



3D-PIC results by A. Pukhov for comparable laser conditions

- ⇒ comparable shape
- ⇒ deviation of absolute numbers (measured density smaller by a factor of 5)

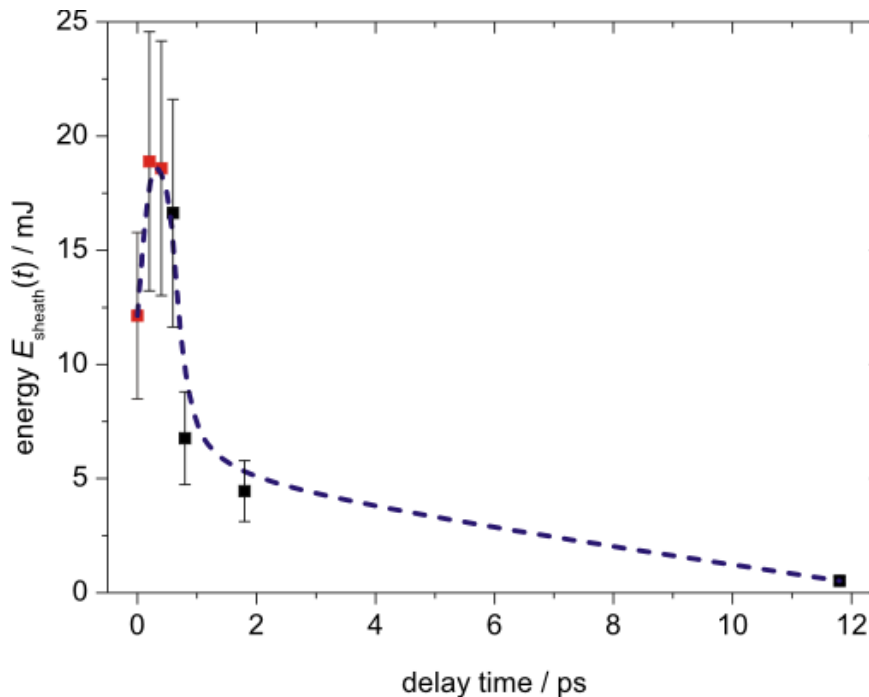
A. Pukhov, PRL **86**, 16 (2001)



# Electromagnetic Probe Pulses

## Probing of laser-driven ion acceleration process

Energy content of electron sheath:  $E_{e^-} = k_B T_e N_e$



Conversion efficiency  $E_{\text{laser}}$   
 $\Rightarrow$  hot electrons:

$$\eta = \frac{E_{e^-}}{E_{L,\text{eff}}} = \frac{k_B T_e N_e}{E_{L,\text{eff}}}$$

$$\eta_{\text{sheath}} = (3.7 \pm 1.2)\%$$

$$\eta_{\text{total}} = (9 \pm 3)\%$$

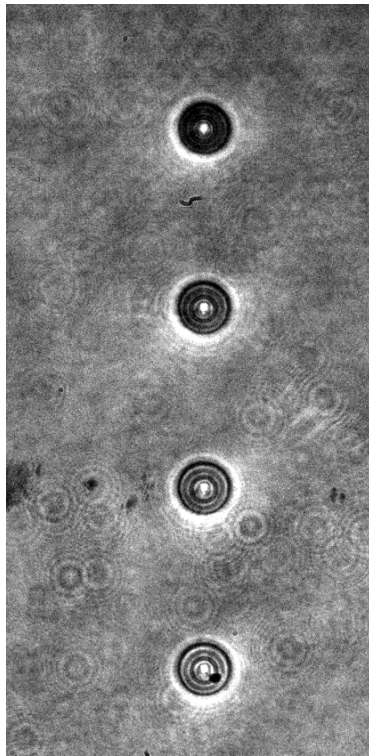
(deduced from sheath's electron density and radial extent, assuming similar hot-e-density inside the target)



# Electromagnetic Probe Pulses

## Probing of droplet targets for laser ion acceleration

Improvement of stability and understanding of acceleration process:  
visualize interaction in the experiment with synchronized probe pulses

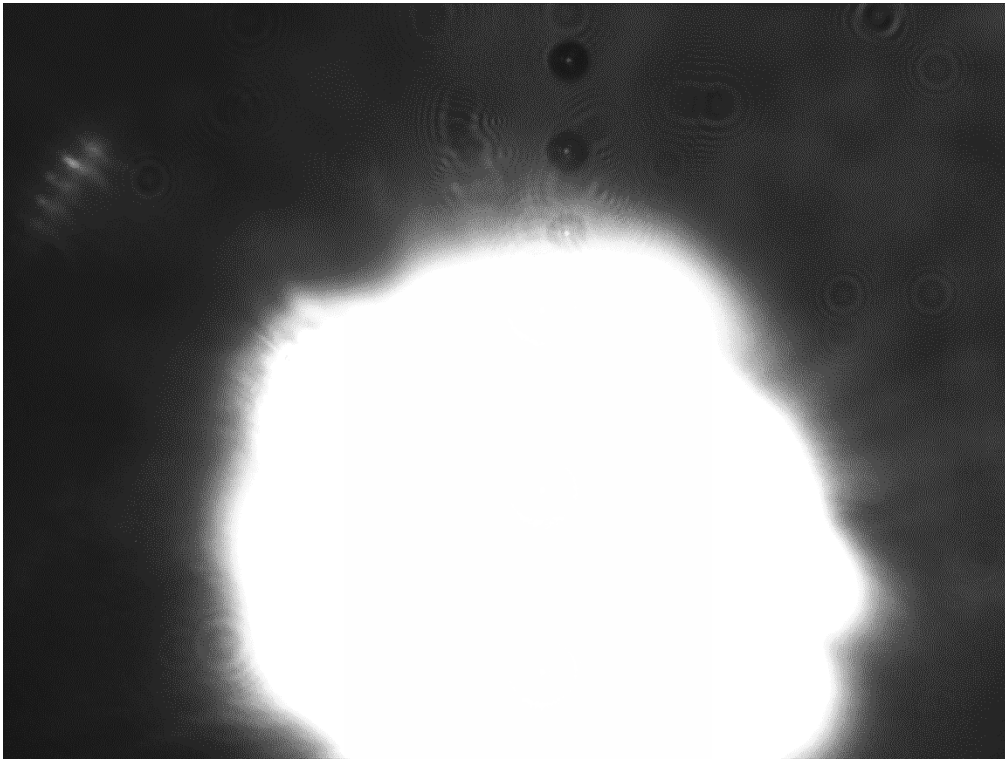




# Electromagnetic Probe Pulses

## Probing of droplet targets for laser ion acceleration

Improvement of stability and understanding of acceleration process:  
visualize interaction in the experiment with synchronized probe pulses



**Problem:**

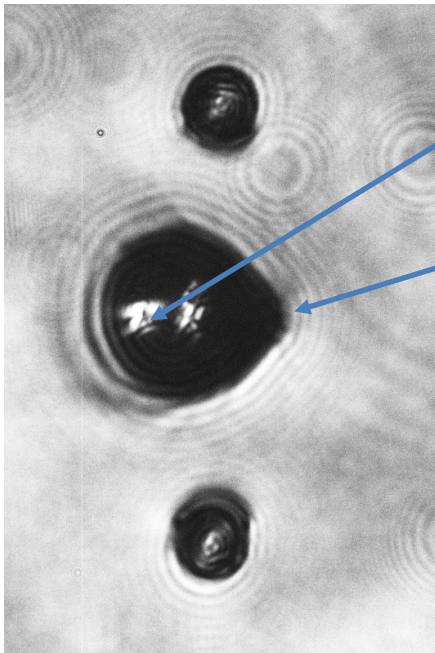
Plasma self-emission outshines  
probe pulse  
⇒ no observation possible!



# Electromagnetic Probe Pulses

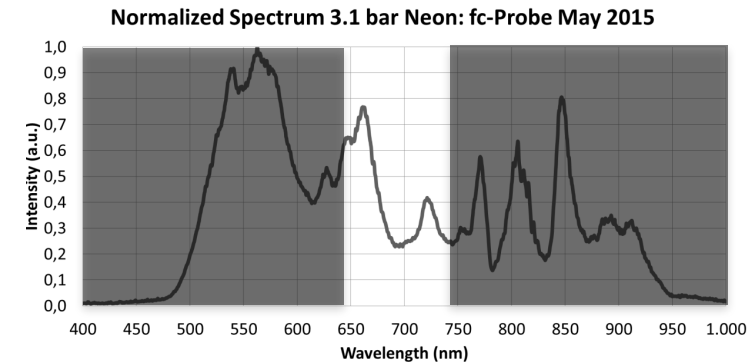
## Probing of droplet targets for laser ion acceleration

Improvement of stability and understanding of acceleration process:  
visualize interaction in the experiment with synchronized probe pulses



Plasma emission strongly suppressed

Droplet expansion (and more)  
can be studied



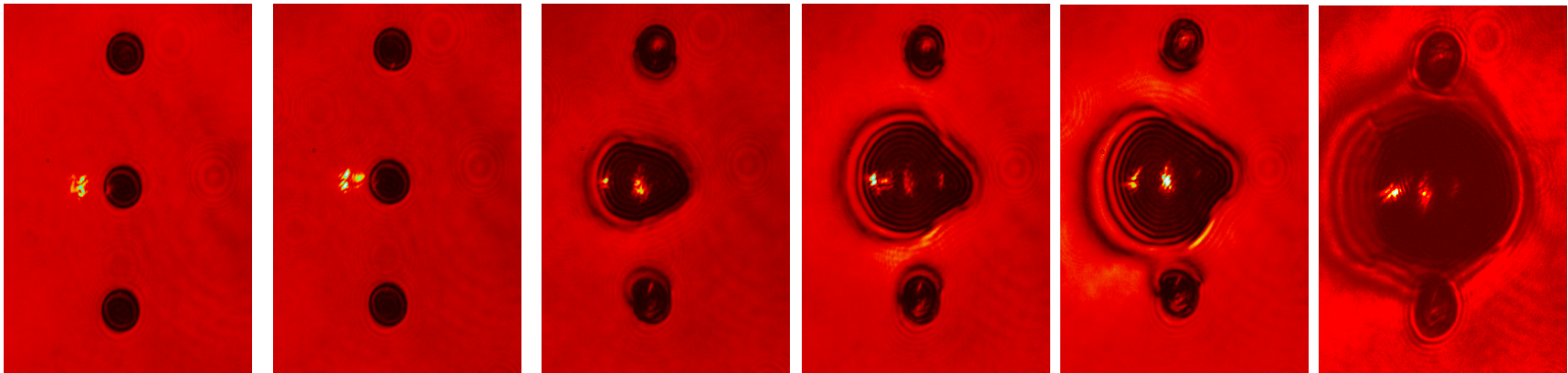
**Solution:** main pulse @ 400 nm, synchronized few-cycle probe pulse @ 710 nm (+ color filter in front of CCD)  $\Rightarrow$  fs- and  $\mu\text{m}$ -resolution



# Electromagnetic Probe Pulses

## Probing of droplet targets for laser ion acceleration

Improvement of stability and understanding of acceleration process:  
visualize interaction in the experiment with synchronized probe pulses



$t_0 + 100 \text{ fs}$

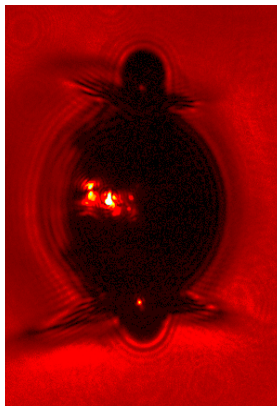
$t_0 + 2 \text{ ps}$

$t_0 + 64 \text{ ps}$

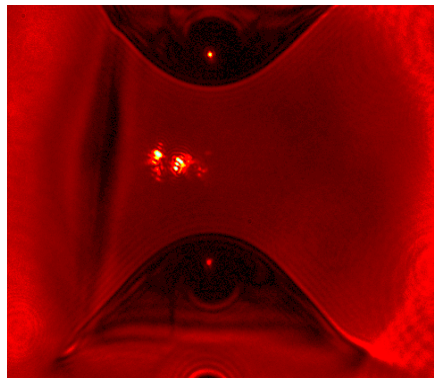
$t_0 + 100 \text{ ps}$

$t_0 + 150 \text{ ps}$

$t_0 + 285 \text{ ps}$



$t_0 + 440 \text{ ps}$



$t_0 + 1.275 \text{ ns}$

- online control of interaction possible,
- influence of focus position on the droplet,
- influence of additional fs-prepulse,
- observation of ion acceleration process,...



# Outline

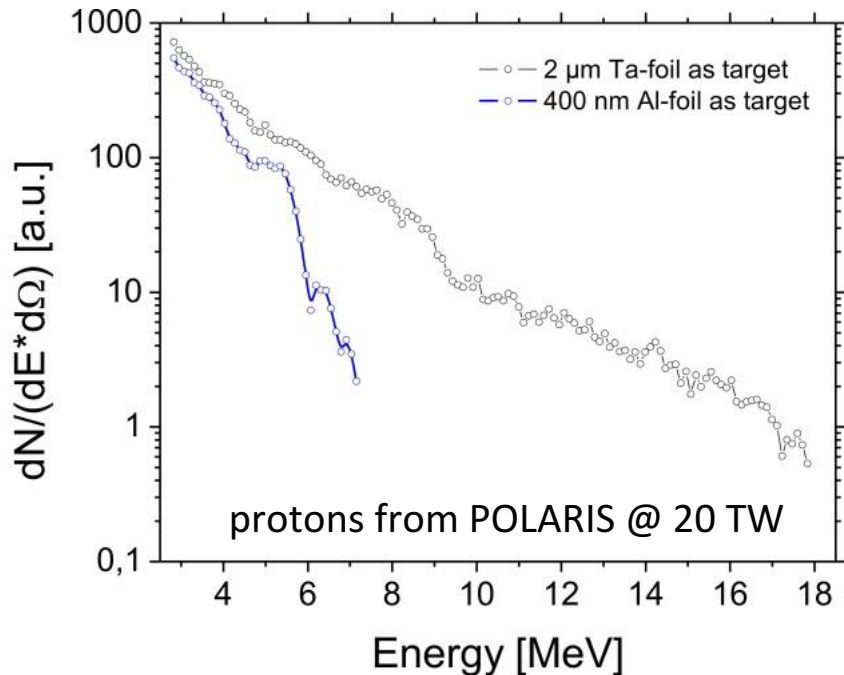
- Motivation: Why plasma diagnostics necessary
- Pump-probe scenarios:  
Which different types of probe pulses can be applied?
- Electro-magnetic probe pulses:
  - Shadowgraphy
  - Interferometry
  - E- and B-field sensitive techniques
- Particle probe pulses:
  - Proton probing
  - Electron probing
  - Detection of magnetic and electric field distributions



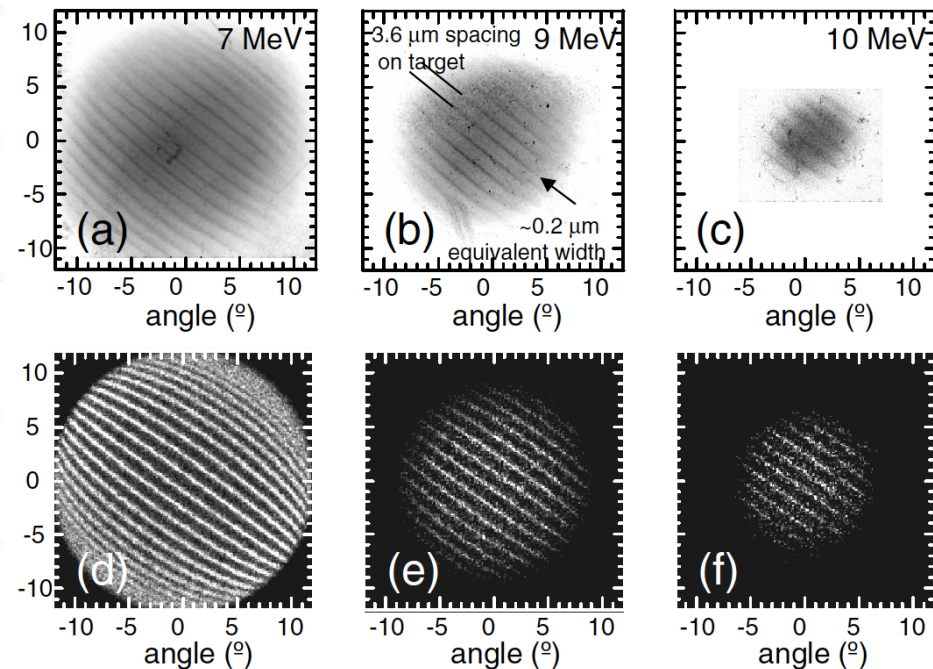
# Particle Probe Pulses

- Probing with laser-accelerated proton beams:
  - broad energy spectrum (up to few 10's of MeV)
  - laminar flow -> excellent imaging properties

Energy spectrum in forward direction



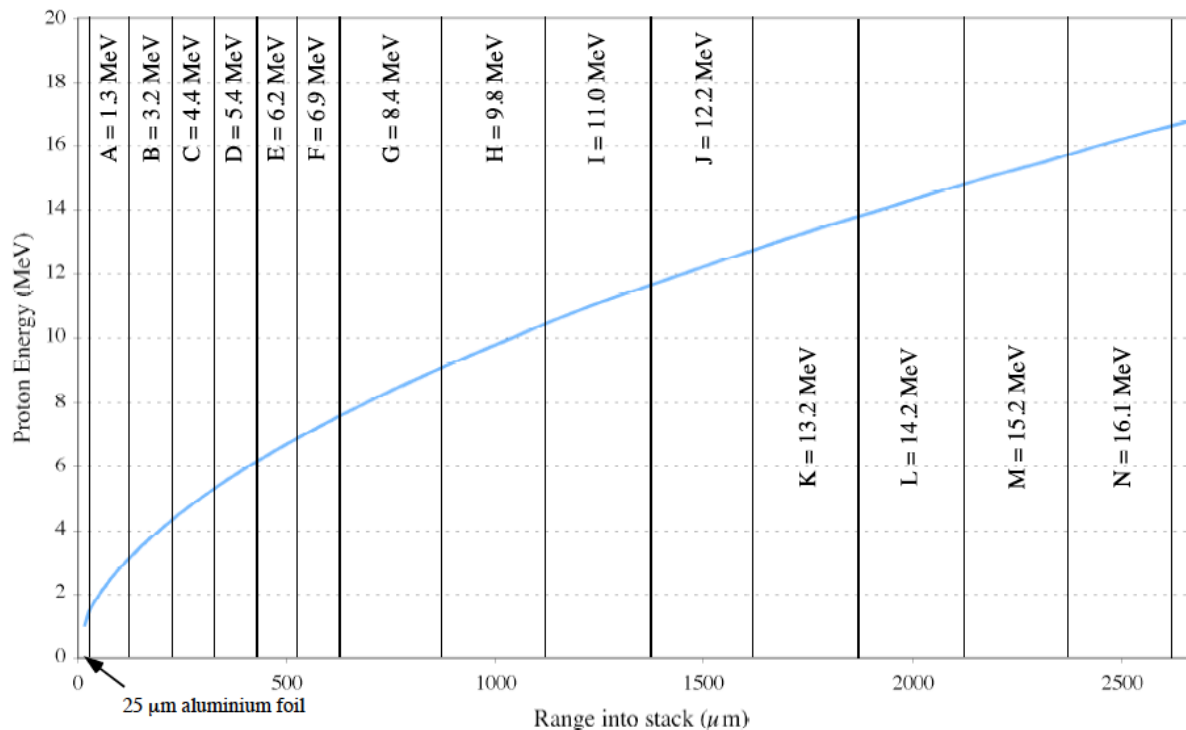
Transverse beam profile for different energies







- Probing with laser-accelerated proton beams:
  - broad energy spectrum (up to few 10's of MeV),
  - laminar flow -> excellent imaging properties
  - energies detected separately in radiochromic film stack



L. Willingale, PhD thesis  
 Imperial College (2007)

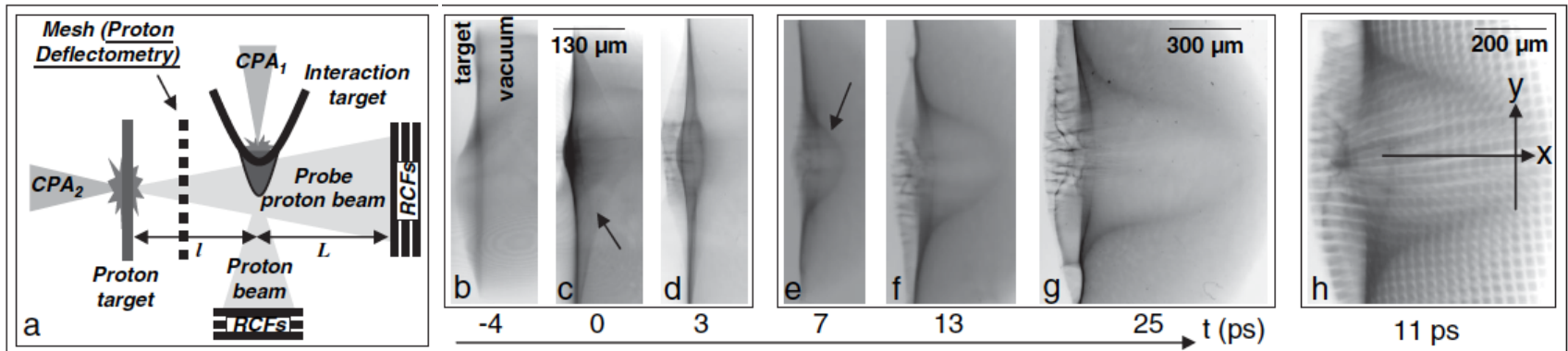


seit 1558

# Particle Probe Pulses

- Probing with laser-accelerated proton beams:
  - broad energy spectrum (up to few 10's of MeV)
  - laminar flow -> excellent imaging properties
  - energies detected separately in radiochromic film stack
  - initial duration  $\approx$  few times laser pulse duration, stretching due to different velocities
- Different images from different proton energies = snapshots from different times during the interaction
- Record movie of evolution of field distribution!

- **Transverse** probing with laser-accelerated proton beams:
  - proton deflection mainly due to electric fields



L. Romagnani, PRL (2005)

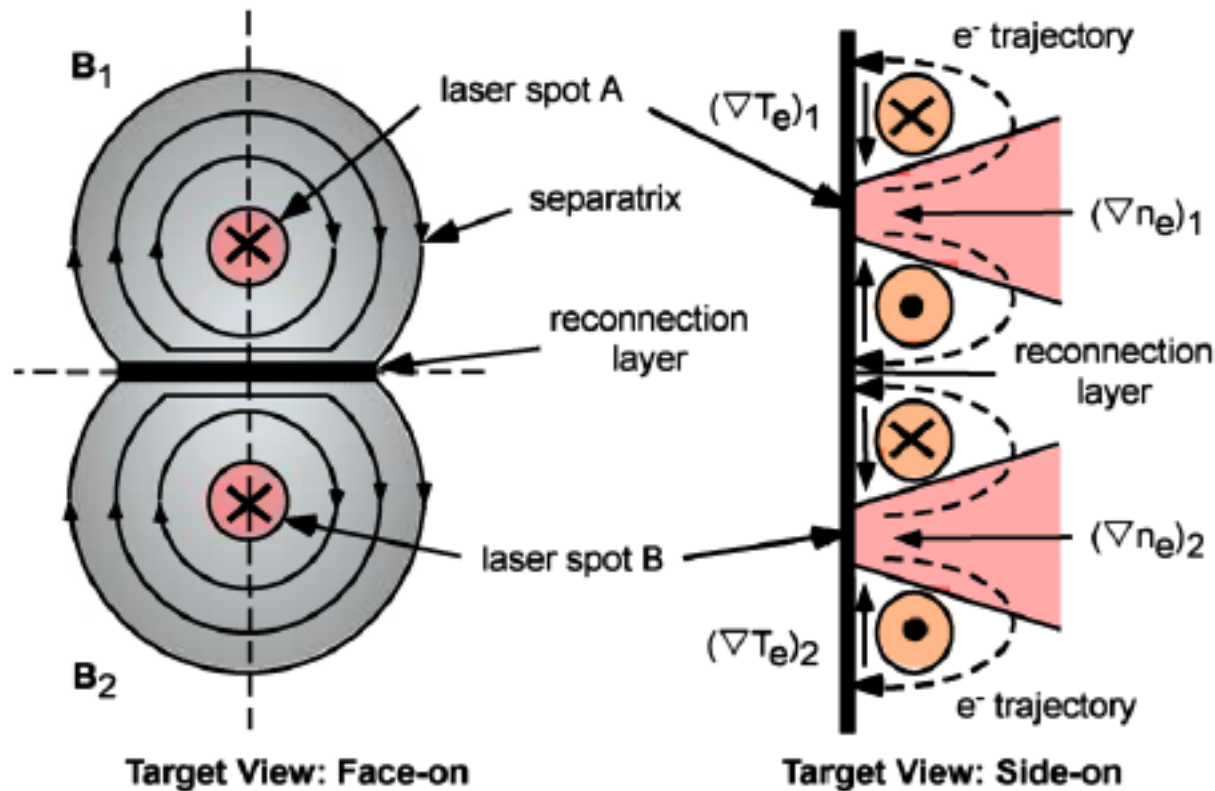
- record TNSA-sheath evolution in single shot,
- deduce sheath-field strength from mesh warping:  
 $E_{\text{TNSA}} \geq 3 \times 10^{10} \text{ V/m}$



seit 1558

# Particle Probe Pulses

- **Longitudinal** probing with laser-accelerated proton beams:
  - proton deflection mainly due to magnetic fields

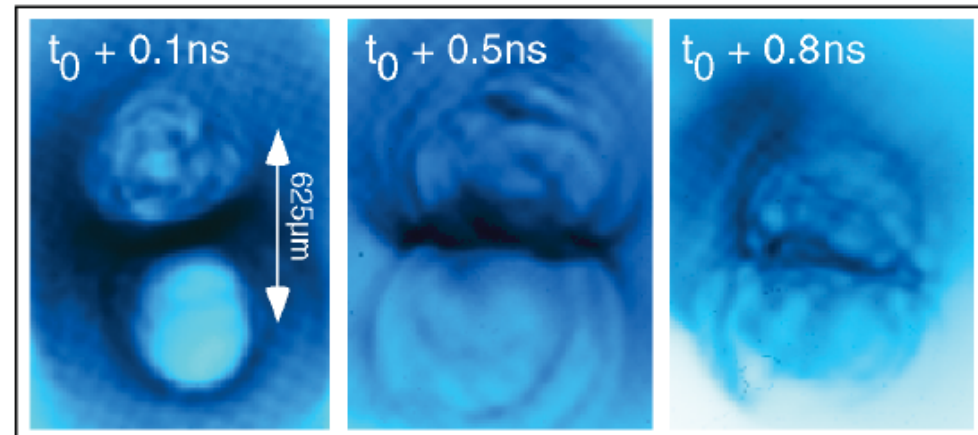
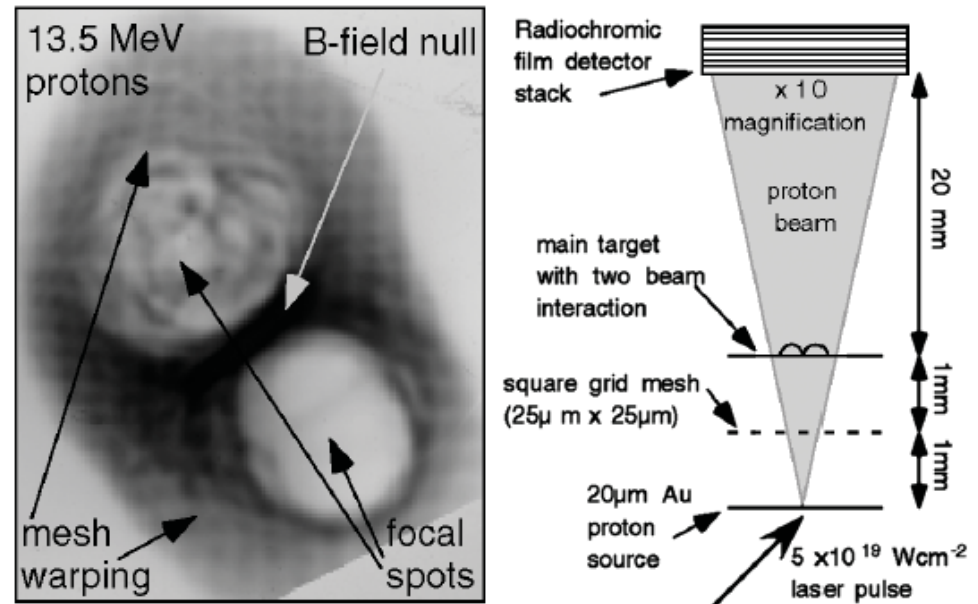




seit 1558

# Particle Probe Pulses

- **Longitudinal** probing with laser-accelerated proton beams:
  - visualize B-field geometry in 2-beam interaction
  - see merging of B-field structures between two plasma plumes
  - example of magnetic reconnection

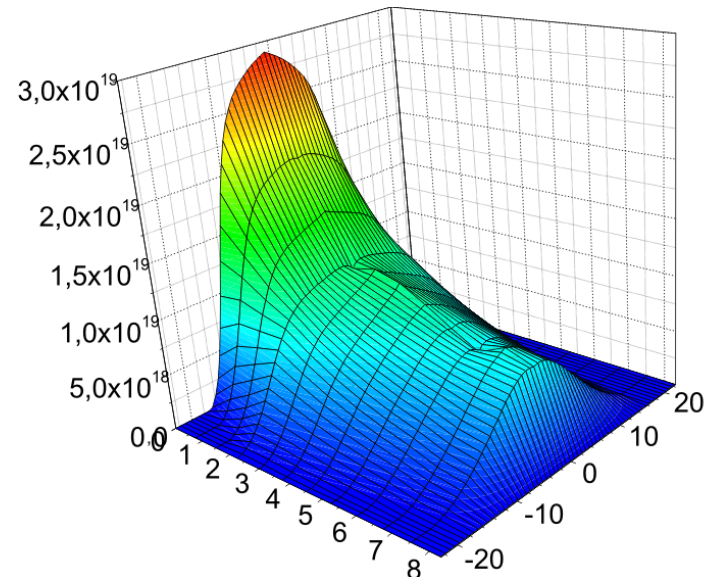
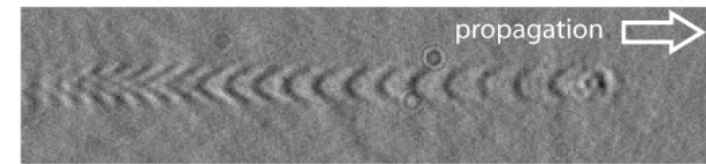
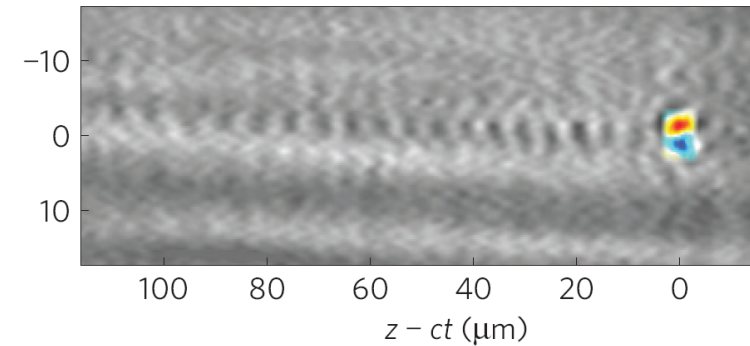




seit 1558

# Conclusions

- Probing diagnostics reveal detailed insight into laser-plasma accelerators
  - Electromagnetic and particle pulses can be used to deduce density and accelerating field distributions in the plasma
  - Accelerating structures (TNSA-sheaths or plasma waves) can be visualized
  - Use of these diagnostics might help to overcome current issues of plasma accelerators (stability/reproducibility) in the future
- ⇒ Further improve plasma diagnostics, their applicability and their resolution in the future!





seit 1558

# Thanks to All Collaborators!



Helmholtz-Institut Jena

A. Sävert, M. Nicolai, M.B. Schwab, M. Reuter, M. Schnell,  
 A. Kawshik, D. Ullmann, H.-P. Schlenvoigt, O. Jäckel,  
 S. Pfoth, J. Polz, J. Heymann, S. Weber,  
 F. Ronneberger, B. Beleites, C. Spielmann, G.G. Paulus  
 Institute of Optics and Quantum Electronics, Friedrich-Schiller-University Jena,  
 Helmholtz-Institute Jena



A. Buck, K. Schmid, C.M.S. Sears, J.M. Mikhailowa,  
 F. Krausz, L. Veisz  
 Max-Planck-Institute of Quantum Optics, Garching

Imperial College  
 London

S.P.D. Mangles, K. Poder, J. Cole, A. E. Dangor,  
 P. M. Nilson, Z. Najmudin  
 Imperial College London, UK



A.G.R. Thomas, L. Willingale, K. Krushelnick  
 Center for Ultrafast Optical Science, Michigan, US



A. Kalinin, R. A. Costa Fraga, R. Grisenti  
 Goethe-University Frankfurt, Germany,  
 GSI Helmholtz Center for Heavy Ion Research, Darmstadt, Germany